Neuron, Vol. 19, 591–611, September, 1997, Copyright ©1997 by Cell Press

Acute Effects of Cocaine on Human Brain Activity and Emotion

Hans C. Breiter,[1,2,9] Randy L. Gollub,[2] Robert M. Weisskoff,[1] David N. Kennedy,[1,3] Nikos Makris,[3] Joshua D. Berke,[5] Julie M. Goodman,[1,2] Howard L. Kantor,[1,6] David R. Gastfriend,[2,4] Jonn P. Riorden,[2,4] R. Thomas Mathew,[2,4,7] Bruce R. Rosen,[1] and Steven E. Hyman[2,8]

[1]Nuclear Magnetic Resonance Center
Department of Radiology
[2]Department of Psychiatry
[3]Center for Morphometric Analysis
Department of Neurology
Massachusetts General Hospital and Harvard Medical School
Boston, Massachusetts 02129
[4]Addictions Services
Department of Psychiatry
Massachusetts General Hospital and Harvard Medical School
Boston, Massachusetts 02114
[5]Program in Neuroscience
Harvard University
Boston, Massachusetts 02115
[6]Department of Cardiology
Massachusetts General Hospital and Harvard Medical School
Boston, Massachusetts 02114

Summary

We investigated brain circuitry mediating cocaine-induced euphoria and craving using functional MRI (fMRI). During double-blind cocaine (0.6 mg/kg) and saline infusions in cocaine-dependent subjects, the entire brain was imaged for 5 min before and 13 min after infusion while subjects rated scales for rush, high, low, and craving. Cocaine induced focal signal increases in nucleus accumbens/subcallosal cortex (NAc/SCC), caudate, putamen, basal forebrain, thalamus, insula, hippocampus, parahippocampal gyrus, cingulate, lateral prefrontal and temporal cortices, parietal cortex, striate/extrastriate cortices, ventral tegmentum, and pons and produced signal decreases in amygdala, temporal pole, and medial frontal cortex. Saline produced few positive or negative activations, which were localized to lateral prefrontal cortex and temporo-occipital cortex. Subjects who underwent repeat studies showed good replication of the regional fMRI activation pattern following cocaine and saline infusions, with activations on saline retest that might reflect expectancy. Brain regions that exhibited early and short duration signal maxima showed a higher correlation with rush ratings. These included the ventral tegmentum, pons, basal forebrain, caudate, cingulate, and most regions of lateral prefrontal cortex. In contrast, regions that demonstrated early but sustained signal maxima were more correlated with craving than with rush ratings; such regions included the NAc/SCC, right parahippocampal gyrus, and some regions of lateral prefrontal cortex. Sustained negative signal change was noted in the amygdala, which correlated with craving ratings. Our data demonstrate the ability of fMRI to map dynamic patterns of brain activation following cocaine infusion in cocaine-dependent subjects and provide evidence of dynamically changing brain networks associated with cocaine-induced euphoria and cocaine-induced craving.

Introduction

Cocaine is one of the most reinforcing drugs known, both in humans and in animals (Johanson and Fischman, 1989). With repetitive use, cocaine may produce a profound state of addiction in humans characterized by compulsive drug use and inability to control use despite significant adverse consequences (Gawin, 1991; American Psychiatric Association, 1994). Progress toward understanding the neural substrates of addiction to cocaine has been substantial in recent years but has been focused on animal models that permit invasive studies. Noninvasive functional neuroimaging approaches, such as functional magnetic resonance imaging (fMRI), now allow studies of neural circuit function to be extended to the human. This has the advantage of being able to correlate subjective information about emotional and cognitive responses with observed patterns of brain activation.

Based on extensive investigations of rodent and primate models, the mesoaccumbens dopamine pathway, extending from the ventral tegmentum of the midbrain (VT) to the nucleus accumbens, appears to be the critical shared substrate of the reinforcing effects of cocaine (Louilot et al., 1989; Williams, 1989; Apicella et al., 1991; Schultz et al., 1992) and other addictive drugs (reviewed in Koob, 1996). Using nondrug stimuli, the nucleus accumbens has also been shown to play a critical role in learning associated with reinforcement (Mirenowicz and Schultz, 1996). Reinforcement in animals depends on the increase in synaptic dopamine levels in the mesoaccumbens circuit produced by cocaine-like drugs via blockade of the dopamine reuptake transporter (DAT) (DeWit and Wise, 1977; Ritz et al., 1987). In both animals and humans, the acutely reinforcing effects of psychostimulant drugs can produce a pattern of repeated self-administration. Human users may initially self-administer cocaine to gain pleasure, to conform to peer behavior, or to relieve stress and other dysphoric feelings. An accelerated pattern of drug use in vulnerable individuals may produce increasing levels of dependence and, eventually, addiction (Hyman, 1996).

While the mesoaccumbens dopamine pathway has been most closely implicated in the acutely rewarding actions of cocaine, other circuits have also been implicated in reward processes, including the basal forebrain, which receives major afferents from the nucleus

[7]Present address: Tri-County Center for Substance Abuse Treatment, Wilmington, North Carolina, 28402.
[8]Present address: Office of the Director, National Institute of Mental Health, Bethesda, Maryland, 20892.
[9]To whom correspondence should be addressed.

accumbens and itself receives dopaminergic input (Heimer et al., 1997). Brain stimulation reward (BSR) experiments have directly implicated the basal forebrain in reinforcement (Rompre and Shizgal, 1986; Shizgal et al., 1989; Arvanitogiannis et al, 1996). The nucleus accumbens is also strongly linked to the amygdala (Ito et al., 1974; Yim and Mogenson, 1982; Russchen et al., 1985; Amaral, et al., 1992), a linkage thought to be important for the formation of stimulus–reward associations (Jones and Mishkin, 1972; Spiegler and Mishkin, 1981; Gaffan and Harrison, 1987; Gaffan et al., 1988). Recently, PET scanning has demonstrated amygdala activation during cocaine craving in abstinent cocaine-abusing subjects relative to normal controls (Childress et al., 1996, Soc. Neurosci., abstract; Grant et al., 1996; Schweitzer et al., 1996, Soc. Neurosci., abstract). Thus, according to current neurobiological models, the nucleus accumbens, amygdala, basal forebrain, and VT are central components of circuitry mediating brain processes underlying reward and memory of that reward.

A number of human studies using cocaine infusions (Fowler et al., 1989; London et al., 1990; Pearlson et al., 1993; Volkow et al., 1997a) and withdrawing subjects (Volkow et al., 1990, 1991, 1992, 1993, 1997b) have implicated the striatum in human cocaine use, withdrawal, and craving. Given the spatial resolution of the techniques utilized, they may not have fully distinguished the dorsal and ventral striatum, in particular the nucleus accumbens. None of these studies reported specific sampling of other regions implicated with reward processes, such as the VT, basal forebrain, or amygdala. Only three of these studies approached the 1–2 min temporal resolution needed to resolve components of cocaine-induced euphoria (Fowler et al., 1989; Pearlson et al., 1993; Volkow et al., 1997a).

To investigate activity in reward circuitry in humans during cocaine infusions and to associate this activity with subjective reports for both cocaine-induced euphoria and postcocaine craving, we used fMRI (Bandettini et al., 1992; Kwong et al., 1992; Ogawa et al., 1992) in conjunction with physiological monitoring and online evaluation of computerized behavioral rating scales. FMRI with a 1.5 T instrument has higher resolution than previous PET and SPECT studies of cocaine effects, permitting investigation of regions with relatively small volume, such as the nucleus accumbens and the amygdala. For these experiments, cocaine-dependent volunteers underwent an unblinded cocaine infusion the night before the fMRI experiment for clinical screening and for training with behavioral assessments on scales of rush, high, low, and craving. During the subsequent double-blind cocaine (0.6 mg/kg) and saline infusions, subjects rated these four scales every 15 s during multiple fMRI acquisitions (Figure 1). Pilot results from this study have previously been presented (Breiter et al., 1996c; Gollub et al., 1996), and data regarding global versus regional cocaine effects is presented elsewhere (Gollub et al., submitted).

Based upon animal data (Koob and Bloom, 1988; Brown et al., 1992; Stein and Fuller, 1992, 1993), we set out to study whether putative brain reward circuitry such as the nucleus accumbens and VT along with other known sites of cocaine binding such as the caudate nucleus would exhibit blood oxygen level–dependent (BOLD) signal changes (Ogawa et al., 1992) for cocaine and not for saline. We were also interested in studying other regions associated with reward and reward-based memory (e.g., basal forebrain and amygdala) and paralimbic structures reported activated in animal studies of acute cocaine administration (Brown et al., 1992; Stein and Fuller, 1992, 1993; Graham and Porrino, 1995; Hammer et al., 1995; Lyons et al., 1996). We predicted that fMRI activation in the nucleus accumbens would be correlated with behavioral reports of cocaine-induced subjective rush and high in dependent subjects. The results in this report will be focused on subcortical limbic structures and paralimbic cortex, though all regions found activated will be discussed in the text and included as a supplemental table available on the Internet.

Results

Clinical and Physiological Data

Seventeen subjects were infused with cocaine while being scanned with fMRI. Scans affected by uncorrectable gross movement were rejected as uninterpretable. Of these 17 subjects, ten had interpretable fMRI data for the cocaine infusions, and ten had interpretable data for the saline infusions after motion correction (seven studies with usable matched infusions).

Following the cocaine infusion (0.6 mg/kg over 30 s), there was an increase in heart rate (HR) within the first minute, while the increase in mean blood pressure (MBP) was slower. Similarly, the drop in end-tidal carbon dioxide ($ETCO_2$) was also slower. Cocaine ($N = 17$) caused the HR to increase rapidly from a preinfusion value of 60 ± 7 beats per minute (bpm) to 79 ± 16 bpm at 2 min postinfusion ($p < 0.0001$), to 82 ± 12 bpm at 5 min postinfusion ($p < 1 \times 10^{-6}$), to 93 ± 14 bpm at 10 min postinfusion ($p < 1 \times 10^{-8}$). Normal sinus rhythm was observed in all subjects throughout the study (Gollub et al., 1996).

MBP rose slightly from 96 ± 12 torr before the infusion to 101 ± 12 torr at 2 min postinfusion ($p < 0.11$, NS), then up to 111 ± 15 torr at 5 min ($p < 0.002$) before starting to slowly decline. The $ETCO_2$ dropped slowly from a baseline of 39 ± 4 mm Hg to 36 ± 4 mm Hg by 10 min ($p < 0.02$). In all subjects scanned, these three measures had returned to baseline by 2 hr, the interinfusion interval (Gollub et al., 1996). Physiologic responses to the 0.6 mg/kg cocaine infusion are in close accord with previously published studies in experienced cocaine abusers (Fischman and Schuster, 1982; Fischman et al., 1985; Foltin and Fischman, 1991).

Plasma samples taken before the first infusion demonstrated absence of residual cocaine at the time of the first infusion in all of the subjects studied. Peak plasma cocaine levels (C_{max}) following the cocaine infusion ranged from 197 to 893 mcg/l with a mean of 388.7 ± 233.0 ($N = 7$ subjects with complete data). The time to peak cocaine plasma concentration varied from 3 to 15 min for subjects in the initial series of experiments (mean $\pm$ SD: 7.6 ± 4.2 min) and the four subjects with interpretable retest experiments (mean $\pm$ SD: 6.0 ± 2.9 min).

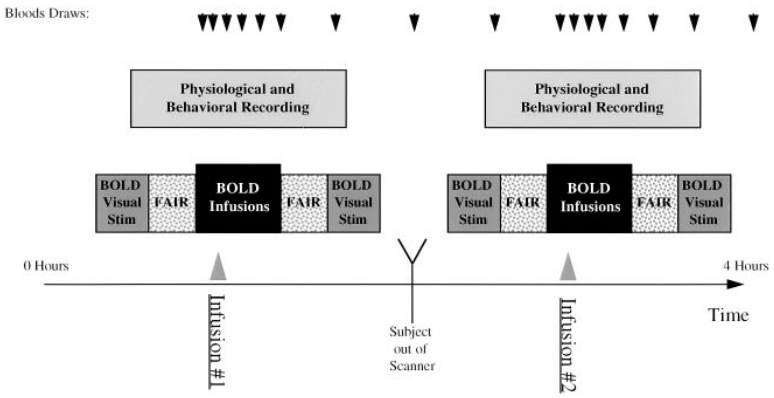

Figure 1. Experiment Design

Over a 5 hr period, subjects participated in ten experimental scans. The experimental runs were grouped, five apiece, around each of the double-blind infusions. Details of each acquisition are presented in Experimental Procedures. Physiological recording along with behavioral ratings were initiated prior to the first FAIR scan and continued through the second FAIR scan of each infusion block. After the first infusion, the second double-blind infusion could not be initiated until the 120 min blood sample had been collected. In between the sets of functional scans for each infusion, clinical scans were acquired for neuroradiolgical assessment. These scans included sagital T1 images, axial proton density and T2 images, and 3-D time-of-flight angiogram.

Scores for the Profile of Mood States (POMS) inventory, assessed before, between, and after the two infusions, showed no change in five of the six POMS measures (i.e., tension, depression, vigor, fatigue, confusion) over the total scan time. Vigor increased in the second infusion for both cocaine and saline infusions. Spielberger scores assessed before, between, and after both infusions indicated no significant change in anxiety levels across scans. These observations would be consistent with the interpretation that subjects did not experience increased discomfort or anxiety in the scanner environment over the course of the experiment.

Behavioral Measures

All ten subjects with interpretable cocaine fMRI data reported clear cocaine effects (see Figure 2). Both peak rush (max score = 3; mean ± SD = 2.2 ± 1.1) and peak high (2.1 ± 0.8) occurred, in the average data, 3 min postinfusion. Peak low (primarily reports of dysphoria and paranoia: 0.9 ± 0.8) occurred 11 min postinfusion, while peak craving (1.3 ± 0.9) occurred 12 min postinfusion. No subject reported effects from the saline infusion on any of the four measures. Ratings obtained for rush, high, low, and craving measures at the 0.6 mg/kg blinded cocaine dosage, given in the fMRI scanner, were higher compared to those obtained at the unblinded 0.2 mg/kg dosage administered in the Massachusetts General Hospital (MGH) Mallinckrodt General Clinical Research Center (GCRC) (rush: 1.2 ± 1.1; high: 1.7 ± 1.2; low: 0.8 ± 0.8; craving: 1.0 ± 1.3). For the four subjects with interpretable test–retest cocaine data, behavioral measures were unchanged on average for the two conditions (retest results, rush: 1.8 ± 1.0; high: 2.3 ± 0.5; low: 1.0 ± 0.8; craving: 1.0 ± 1.2).

Cocaine Infusion

Foci of Signal Change

Cocaine caused regional signal increases (Kolmogorov-Smirnov, $p < 7.1 \times 10^{-6}$) (see Tables 1–4 for multiple limbic and paralimbic regions, supplemental Table 6 http://www.neuron.org/cgi/content/full/19/3/591/T6, and Figures 3a and 3b) in discrete foci in the nucleus accumbens/subcallosal cortex (NAc/SCC), caudate nucleus,

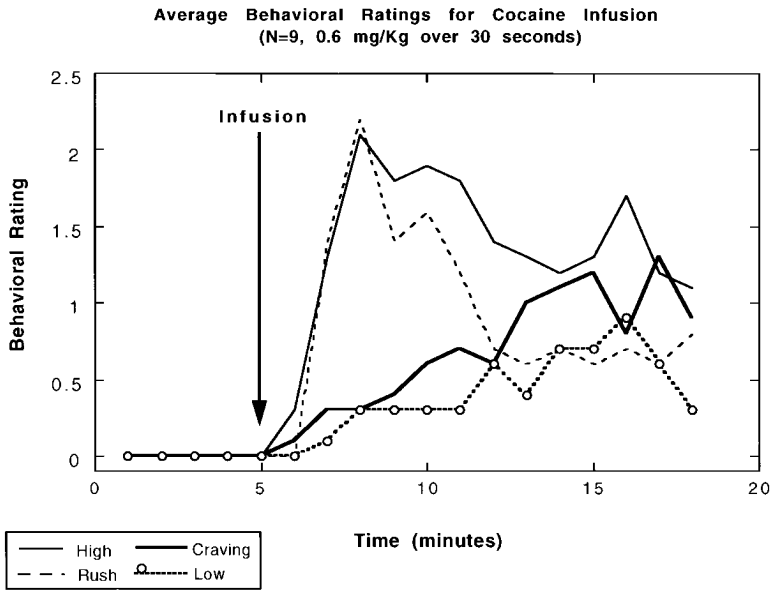

Figure 2. Graph of Average Behavioral Measures

The rush, high, low, and craving ratings were averaged within category for the nine of ten subjects who had interpretable cocaine fMRI data after motion correction and behavioral ratings time-locked to the scanner.

Table 1. Characterization of Cocaine Effects on FMRI Signal in Subcortical Gray Structures

Anatomic Region		Tal Coordinates R/L	A/P	S/I	P Value (KS Statistic)	% Signal Change (Pre versus Post Drug)	Proportion Individuals ($p < 0.001$)	Multiple Correlation Analysis Rush	Craving
NAc/SCC	R	6	7	−9	7×10^{-6}	1.5	9/10	ϕ	+
	L	−6	13	0	4×10^{-6}	1.5	8/10	ϕ	+
Caudate	R	13	−3	22	5×10^{-7}	0.8	8/10	+	−
	L	−9	−3	19	3×10^{-7}	1.0	7/10	+	ϕ
Putamen	R	28	7	−3	4×10^{-8}	1.4	8/10	+	−
	L	−28	7	−3	NS (5×10^{-5})	0.5	5/10	ϕ	ϕ
BF/GP	R	22*	1*	−6*	NS	ϕ	6/10	ϕ	+
	L	−19	0	−3	6×10^{-9}	1.8	7/10	+	−
Thalamus									
aThal	R	3	−18	13	6×10^{-8}	0.4	8/10	ϕ	ϕ
	L	ϕ	ϕ	ϕ	NS	ϕ	7/10	ϕ	ϕ
pThal	R	6	−25	16	9×10^{-7}	1.4	8/10	+	ϕ
	L	−6*	−31*	9*	NS	ϕ	8/10	+	ϕ
LGN	R	19	−25	0	NS (8×10^{-5})	0.8	8/10	+	ϕ
	L	−19	−25	−3	2×10^{-7}	0.5	7/10	+	ϕ

Table 2. Characterization of Cocaine Effects on FMRI Signal in Temporal Lobe

Anatomic Region		Tal Coordinates R/L	A/P	S/I	P Value (KS Statistic)	% Signal Change (Pre versus Post Drug)	Proportion Individuals ($p < 0.001$)	Multiple Correlation Analysis Rush	Craving
Hippocampus									
aHip	R	28*	−18*	−9*	NS	ϕ	9/10	ϕ	−
	L	−28*	−17*	−16*	NS	ϕ	10/10	ϕ	±▽
pHip	R	34	−28	−13	2×10^{-8}	1.8	9/10	+	+
	L	−22	−37	0	NS (1×10^{-5})	0.9	10/10	+	ϕ
Insula									
aINS	R	34	13	6	3×10^{-8}	0.9	10/10	+	ϕ
	L	−28	19	−6	5×10^{-6}	0.5	8/10	+	ϕ
pINS	R	41	−15	0	2×10^{-9}	1.1	8/10	+	ϕ
	L	−41	−12	−3	3×10^{-11}	1.0	7/10	+	+
Amygdala	R	22	−6	−13	NS (-7×10^{-5})	−1.2	4/10 (+), 5/10 (−)	ϕ	−
	L	−25	−9	−19	-1×10^{-6}	−0.3	3/10 (+), 5/10 (−)	ϕ	−

Table 3. Characterization of Cocaine Effects on FMRI Signal in Medial Paralimbic Cortices

Anatomic Region		Tal Coordinates R/L	A/P	S/I	P Value (KS Statistic)	% Signal Change (Pre versus Post Drug)	Proportion Individuals ($p < 0.001$)	Multiple Correlation Analysis Rush	Craving
Cingulate G.									
aCG (BA 24/32)	R	9	13	34	1×10^{-8}	0.9	9/10	+	ϕ
(BA 32)	R	3	26	28	3×10^{-7}	0.8		+	ϕ
(BA 24)	B	0	−3	31	3×10^{-8}	1.0	9/10	+	+
pCG (BA 31)	R	3	−31	38	3×10^{-6}	0.5	8/10	+	ϕ
(BA 31)	L	−9	−28	41	NS (1×10^{-5})	0.5	5/10	+	+
Parahippocampal G.									
(BA 28)	R	22	−21	−22	6×10^{-6}	2.7	9/10	+	++
(BA 28)	L	−19	−28	−9	2×10^{-8}	0.5	9/10	+	+
(BA 35)	R	16*	−40*	−6*	NS	ϕ	ϕ	+	ϕ
(BA 19)	L	−30*	−50*	2*	NS	ϕ	ϕ	+	+

Table 4. Characterization of Cocaine Effects on FMRI Signal in Brainstem

Anatomic Region		Tal Coordinates R/L	A/P	S/I	P Value (KS Statistic)	% Signal Change (Pre versus Post Drug)	Proportion Individuals ($p < 0.001$)	Multiple Correlation Analysis Rush	Craving
VT (SN)	R	9	−15	−13	4×10^{-6}	1.1	6/10	+	ϕ
	L	−16	−21	−6	3×10^{-9}	1.5	6/10	+	ϕ

putamen, basal forebrain, thalamus, insula, hippocampus, parahippocampal region, cingulate, lateral frontal cortices, lateral temporal cortex, parietal cortex, striate and extrastriate cortices, along with regional decreases in signal in amygdala (see Tables 1–4 and Figure 3b), temporal pole, and medial frontal cortex (see supplemental Table 7 http://www.neuron.org/cgi/content/full/19/3/591/T7). Negative activation in the temporal pole and medial frontal cortex lay in close proximity to regions of susceptibility artifact. Positive signal change was also noted in the vicinity of the VT and the pons.

Across most positive and negative activations with cocaine, plots of signal intensity versus time showed early signal maxima with rapid (starting within 1 min of the signal maxima) decrease toward baseline. Some activations, however, demonstrated early signal maxima that were sustained at a plateau level for time periods ranging from 5 min to the end of the scanning interval. These differences in time course appeared to correlate with different behavioral states.

Large activations in a few individuals may result in statistically significant activations in the averaged group data. To determine the extent to which the averaged data reflects common activations, statistical maps were analyzed for 16 subcortical regions (see Figure 4 for examples of anatomic definitions and Tables 1–4 for results) in the ten subjects used for the average map. The data is presented as the ratio of the number of subjects who showed activation in that structure at a less stringent p value threshold ($p < 0.001$); this type of analysis has previously been reported (Breiter et al., 1996b). The individual data analysis strongly supports the average results in the NAc/SCC, thalamus, hippocampus, insula, cingulate gyrus, and parahippocampal gyrus with eight or nine of ten subjects contributing to the group activation. Other regions including caudate, putamen, basal forebrain, and VT also reflected majority activation with six to eight subjects showing activation. One exception was noted: the amygdala demonstrated response heterogeneity across individuals. This heterogeneity suggests caution in the interpretation of the negative amygdala activation in the average map.

Correlation Maps

Multiple correlation analysis was used to determine whether activations observed for the baseline versus postinfusion comparison were associated with specific behavioral states. We calculated a correlation value (R) for each behavioral measure to describe the strength of similarity between the signal time course of each brain voxel to that behavioral measure. We used a multiple correlation technique with the rush and the craving ratings, because these measures were the most temporally distinct from each other (see Figure 2). Namely, rush ratings had early and transient maxima, while craving ratings had a longer latency to reaching maximum following infusion. The resulting correlation data are shown in Tables 1–4 and in Figure 5.

Regions that correlated with rush had early and transient signal maxima. Strong correlations were noted for the left basal forebrain and bilateral VT. In addition, many other regions of brain activation on our KS maps due to cocaine were positively correlated with rush ratings, including sections of the right cingulate gyrus, bilateral insula, bilateral thalamus, bilateral caudate nucleus, bilateral pontine brainstem, and the majority of activations in the prefrontal cortex.

Regions that showed significant correlation with craving had early signal maxima (or minima for the negative activations) followed by sustained signal change. The sustained signal change (see Figures 3a and 3b) in these regions produced the strong correlation with craving. Thus, while regions hypothesized to be involved in brain reward (NAc/SCC) and reinforcement-based memory (amygdala) showed signal changes (positive and negative changes, respectively) early, at the time of subjective rush and high, both regions showed persistent signal changes that correlated significantly with subjective reports of craving and not rush. Another region that showed a positive correlation with craving was a region of the right parahippocampal gyrus.

Finally, other regions demonstrated significant correlation with both rush and craving ratings, identified in Tables 1–4 by a plus sign in the columns for both ratings. Of these regions, those that overlapped with activations

---

Tables 1–4 summarize activation due to cocaine infusion. Anatomic Region identifies the structure on the basis of subcortical location, lobe, gyrus (if medial paralimbic cortex), or placement in the brainstem. See Experimental Procedures for details regarding anatomic definitions and localization. BA indicates the probable Brodmann area, for cortical areas, of activation in the group average data as determined from the atlas of Talairach and Tournoux (1988). Activation laterality is denoted by R and L; when bilateral, a B is used. Tal Coordinates denotes the Talairach coordinates using the atlas of Talairach and Tournoux (1988) of the voxel with the maximum p value for the KS maps of pre- versus postinfusion time points and overlapping correlation regions (except where denoted by an asterisk, in which case the coordinates denote the location of the voxel with maximum p value for the correlational analysis when no significant activation was present in the KS maps of the group average data). Coordinates are expressed in mm from the anterior commissure: R/L, right (+)/left (−); A/P, anterior (+)/posterior (−); S/I, superior (+)/inferior (−). P value indicates the maximum p value for each activated cluster of voxels on the unsmoothed Kolmogorov-Smirnov statistical map. Regions are listed as significant if $p < 7.1 \times 10^{-6}$ (see Experimental Procedures). When NS (nonsignificant) is followed by a p value in parentheses, this indicates a region of activation that did not meet our significance threshold, yet due to symmetric placement with respect to another activation in the opposite hemisphere was included. Percent signal change was determined for each activation by taking all voxels around the max vox with $p < 10^{-5}$ and comparing the first 38 fMRI time points with the subsequent 98 time points. Proportion Individuals lists the number of subjects to the total number of subjects ($N = 10$) who showed activation ($p < 10^{-3}$ for each voxel) in each anatomically defined region of interest; these regions of interest may include one or more activations from the group average statistical analysis. Correlation Analysis lists the results of a multiple correlational analysis of the fMRI time data to the behavioral measures of rush and craving. A plus sign indicates a positive correlation, a minus sign indicates a negative correlation, and a ϕ indicates no correlation to the measure. To be tabulated, a correlation region had to have five voxels with $R > 0.70$ for each voxel (see Experimental Procedures). The symbol $\pm$ indicates two nearby correlation regions of opposite sign in the same anatomic region. In Table 3, note that two plus signs are placed in the craving column for one activation; in this case, one correlation region was correlated to similar degree with both rush and craving measures, while the other correlation region was uniquely correlated to craving alone.

a

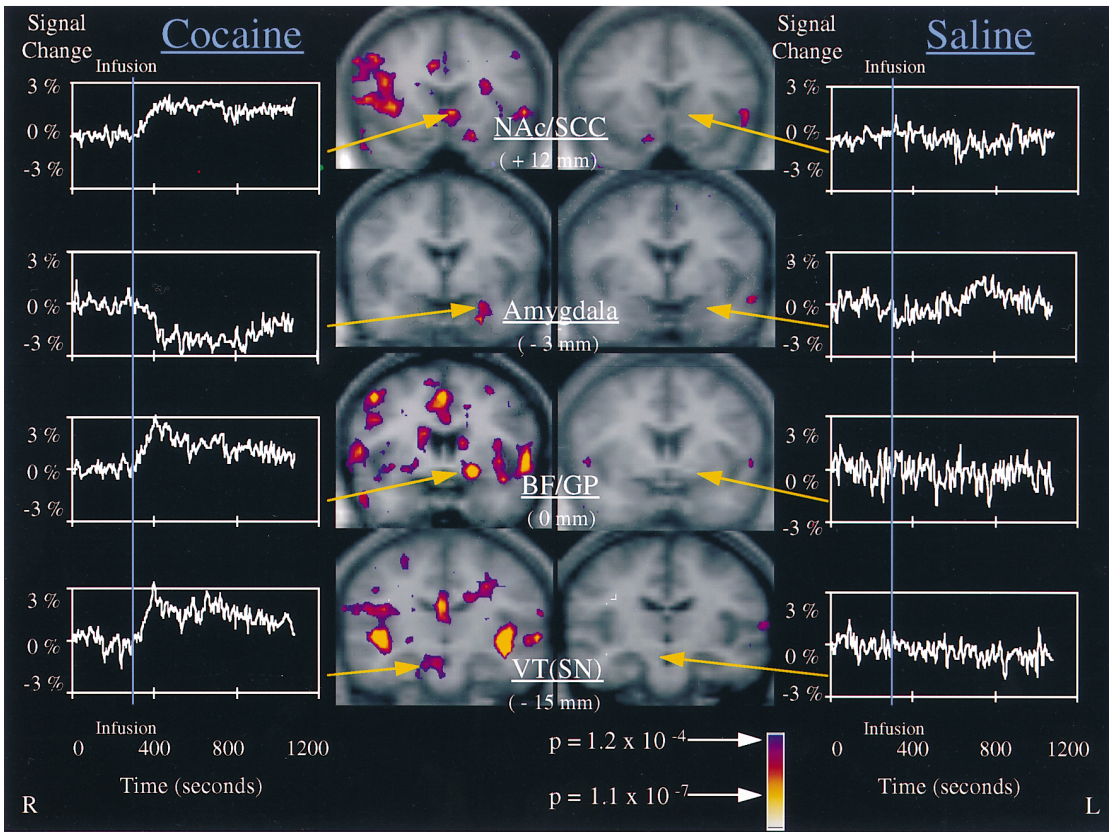
Signal Change
Cocaine
Infusion
3 %
0 %
-3 %
NAc/SCC
(+ 12 mm)
Amygdala
(- 3 mm)
BF/GP
(0 mm)
VT(SN)
(- 15 mm)
Signal Change
Saline
Infusion
0
400
800
1200
Time (seconds)
p = 1.2 x 10 -4
p = 1.1 x 10 -7
R
L

b

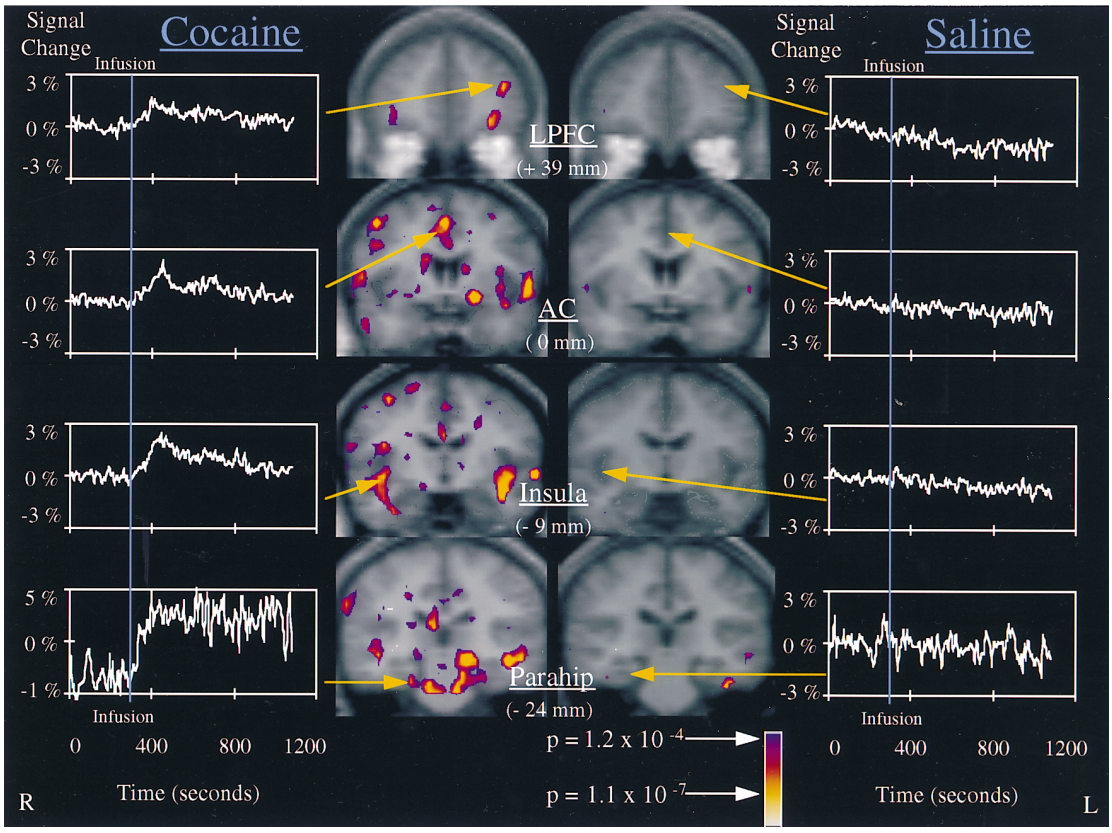
Signal Change
Cocaine
Infusion
3 %
0 %
-3 %
LPFC
(+ 39 mm)
AC
(0 mm)
Insula
(- 9 mm)
Parahip
(- 24 mm)
5 %
-1 %
Signal Change
Saline
0
400
800
1200
Time (seconds)
p = 1.2 x 10 -4
p = 1.1 x 10 -7
R
L

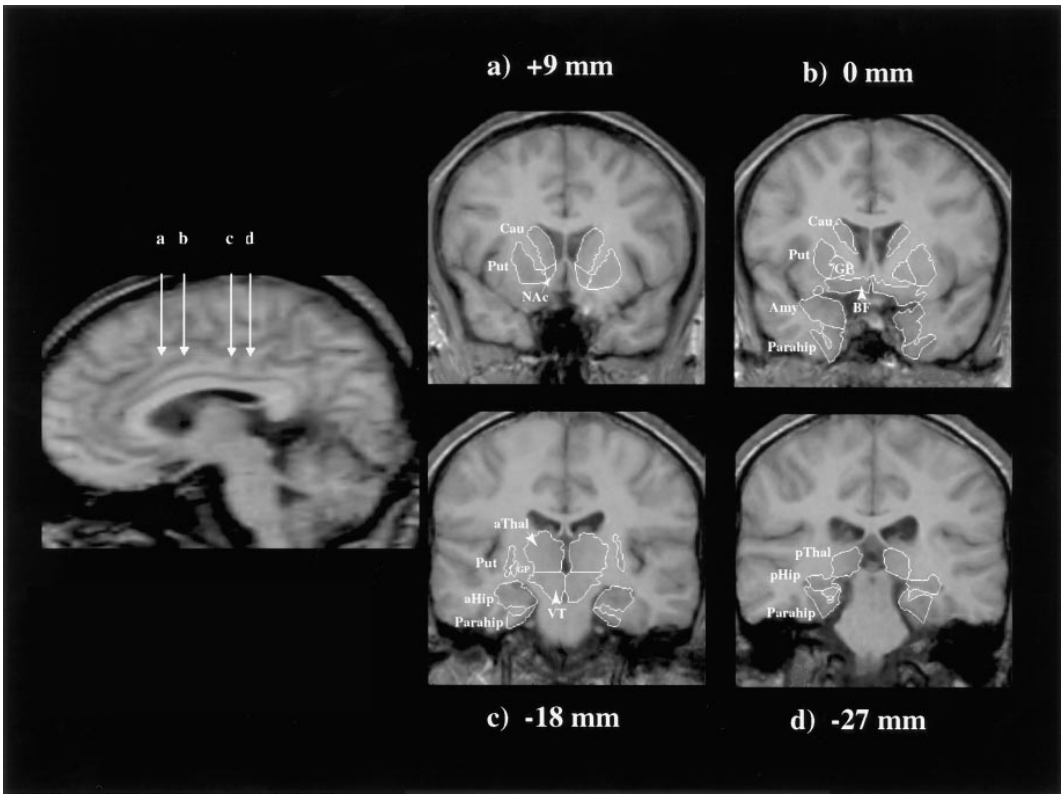

Figure 4. Selected Anatomic Definitions Used for Average and Individual Activation Localization

Structural T1 images from one individual are shown in the same orientation as the Talairach coronal position. Regions of interest for localization of statistical map activations are indicated in white on top of these gray scale structural images. Coronal slice planes are given with respect to the anterior commissure. The abbreviations and definitions used in this image are defined in the Expermental Procedures section on anatomic localization of activations. It has to be pointed out that the nucleus accumbens (NAc in the figure) can be distinguished on this individual's image from the subcallosal cortex that is adjacent and medial to it. This distinction between nucleus accumbens and subcallosal cortex is not possible on averaged images and is not always possible on individual images. Therefore, we refer to a nucleus accumbens/subcallosal cortex region of interest for both our averaged data and our individual data.

seen in the comparison of preinfusion versus postinfusion time points include sections of the left parahippocampal gyrus, left cingulate gyrus, left insula, and right hippocampus.

Test–Retest Comparisons

Seven subjects had retest infusions at times ranging from 3.5 to 4 months after the first experiment. Of these seven, four subjects had interpretable cocaine infusion data after motion correction for test–retest comparison. These four subjects received their double-blind cocaine and saline infusions in the same order for the retest experiments as for the test experiments. To keep expectancies as similar as possible between test and retest conditions, subjects had been informed on several occasions that the identity of the first retest infusion did not imply the identity of the second retest infusion and that the MGH pharmacy maintained a double-blind experimental design for subjects and researchers during all retest infusions. Regions of positive signal change that were similar between average maps of the test and retest cocaine infusions are listed in Table 5. Note that activations that overlapped did not necessarily have statistical maxima in the exact same anatomic region. However, their statistical maxima were within 1.5 cm of each other or the two activation clusters had overlapping voxels at a high statistical threshold. Twenty-six of

Figure 3. Regional Brain Activation with Cocaine and Saline

(a) Images of subcortical brain regions showing significant fMRI signal changes after cocaine, but not after saline, infusions. On the left are Kolmogorov-Smirnov (KS) statistical maps at four coronal levels of pre- versus postinfusion time points for the average fMRI data from ten subjects who received cocaine. These KS statistical maps are overlaid in pseudocolor on corresponding gray scale average structural maps. Activations with positive signal change include the NAc/SCC, BF/GP, and VT, while activations with negative signal change include the amygdala. The signal intensity versus time graph for the activations (for all voxels with $p < 10^{-6}$ within the named region) is placed next to each image. On the right are identical slice planes overlaid with the KS statistical map for the saline infusion; the saline signal intensity versus time graphs for the same anatomic regions active during cocaine are placed next to the saline images to demonstrate the absence of comparable change.

(b) Images of other paralimbic and heteromodal cortex activations after cocaine and after saline infusions. Regions shown include the lateral prefrontal cortex (LPFC), anterior cingulate, insula, and parahippocampal gyrus. Image and graph layout follow the conventions described in (a).

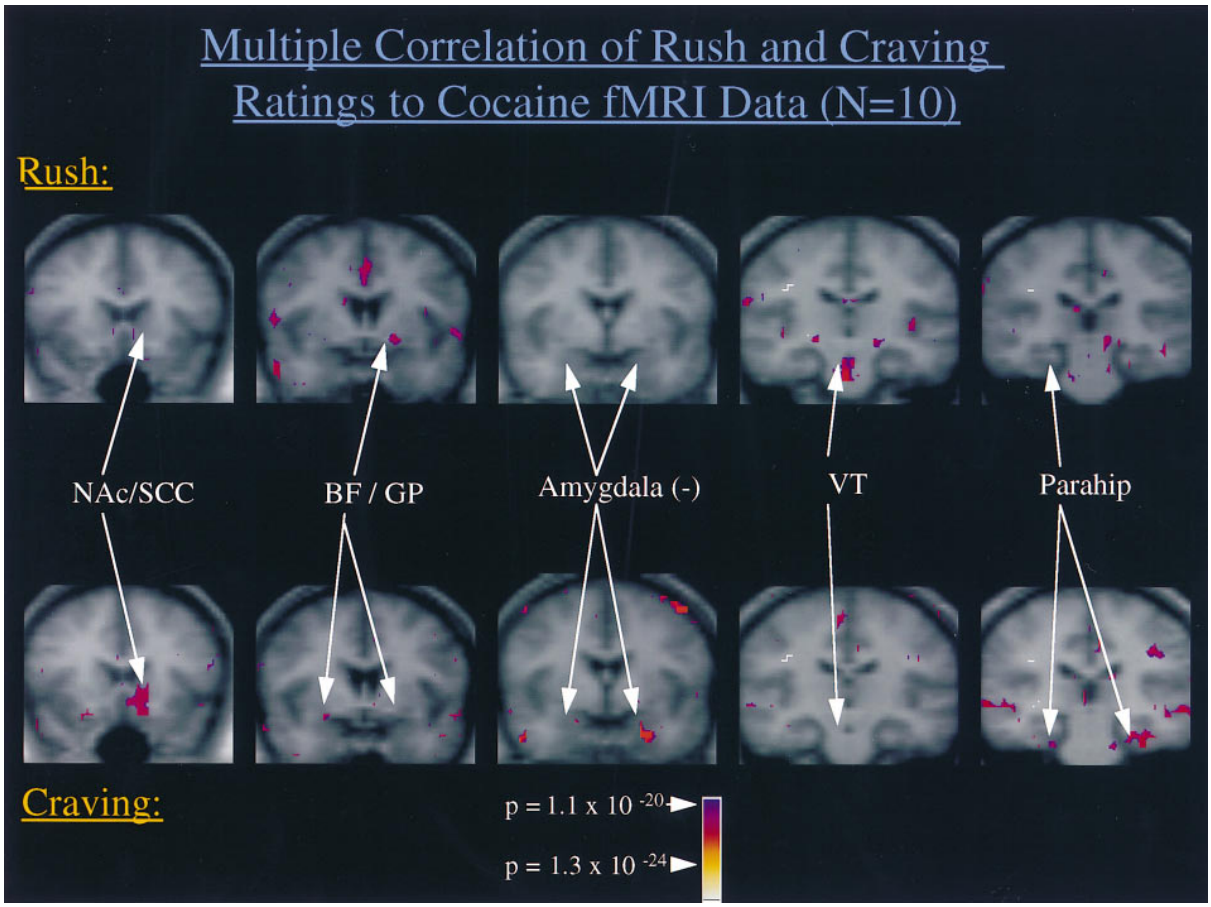

Figure 5. Multiple Correlation Images

Correlation images associated with rush and with craving are displayed as coronal images, respectively, in the top row and the bottom row. Each correlation map is presented as a pseudocolor p value map superimposed on a gray scale structural image. Coronal images represent slices from +15 mm, 0 mm, −3 mm, −18 mm, and −24 mm with respect to the anterior commissure. Regions highlighted in this figure were more strongly correlated with one behavioral measure than another and include the NAc/SCC, BF/GP, Amygdala, VT, and parahippocampal gyrus.

thirty-two postcocaine activations in the test sample were matched by similar activations in the retest experiments, including subcortical regions originally hypothesized to be activated, namely the NAc/SCC (see Figure 6), basal forebrain, and caudate. For regions such as the NAc/SCC, the percent signal change for voxels meeting the threshold of $p < 10^{-5}$ in the test condition (left = 3.8%, right = 2.4%) was marginally higher than the percent signal change for the retest condition (left = 2.3%, right = 2.1%), though more voxels met the $p < 10^{-5}$ threshold on retest.

Other areas of activation that matched between test and retest conditions included parahippocampal regions, thalamic, insular, and cingulate regions. For the average map of four subjects in the test condition, there were fewer activations overall (N = 32) than for the average map with ten subjects (N = 92 activations with positive signal change). This raises the possibility that the smaller cohort had insufficient power to identify smaller magnitude signal changes, thus the test cohort's activation profile may be a subset of the larger group's activation profile. In support of this possibility is the observation that of the 56 regions observed with the cocaine retest experiment, 28 regions were not matched by previous test activations, but 22 of these directly matched activations seen with the total cohort of ten subjects. Other factors that might contribute to the heterogeneity include the current level of cocaine usage or altered anxiety or positive expectancy related to the prior experience with our experimental procedures.

Saline Infusion

Foci of Signal Change

In the ten subjects with interpretable data, saline infusions produced no positive signal change in limbic or paralimbic regions. One focus of negative signal change was noted in the left temporal pole, which approximated a similar activation for the cocaine infusion. For areas outside of limbic and paralimbic regions, positive signal changes were noted in the inferior frontal gyrus, inferior/middle temporal gyri, and extrastriate region (see supplemental Table 8 http://www.neuron.org/cgi/content/full/19/3/591/T8) and negative signal changes in lateral frontal cortex, superior temporal gyri, and extrastriate cortex (see supplemental Table 9 http://www.neuron.org/cgi/content/full/19/3/591/T9). All five positive activations with saline matched the location of activations

Table 5. Test–Retest Cocaine Infusions: Regions of Similarity for Foci of Positive Signal Change

Test						Retest					
Anatomy (Region/BA)	Tal Coordinate R/L	A/P	S/I	Vox #		Anatomy (Region/BA)	Tal Coordinate R/L	A/P	S/I	Vox #	Proximity (<1.5 cm)
Subcortical Gray Structures											
Caudate/NAc	25	−27	18	8		Caudate	18	−12	21	77	−
Caudate/NAc	9	15	−3	81		GO a11	3	15	−6	160	+
BF/GP	−21	0	−6	10		BF/GP	−15	3	0	23	+
Thalamus/pThal	6	−27	12	62		Caudate	18	−12	21	77	−
						Cingulate a23	3	−27	28	43	−
Temporal Lobe											
Lateral and Intrasylvian Surfaces											
GTm a21	43	−6	−15	28		GTm a21	46	−18	−9	26	+[a]
Insula	37	−15	−3	38							+
Insula	−40	−15	−6	129		Insula	−40	−9	0	63	+
						GTm a21	−46	−24	−3	57	+
Insula	−40	6	0	45		Insula	−40	−9	0	63	+
Insula	−34	12	18	12		Insula	−37	18	6	66	+[a]
Medial Paralimbic Cortices											
Cingulate a24	0	−3	40	8		Cingulate a24	3	9	34	83	+
Cingulate a23/31	21	−27	34	13		Cingulate a23	12	−18	34	18	+
						Cingulate a23	3	−27	28	43	−
Parahip a35	18	−36	−12	89		GF a37	46	−51	−21	152	−
						GF a20/36	34	−33	−15	26	+[a]
Parahip a28/36	−21	−24	−21	83		Thalamus/pThal	−18	−15	3	17	−
						Parahip a35/36	−28	−27	−15	150	+

Table 5 shows which activations were similar between test and retest conditions for the cocaine infusions. Specific anatomic regions are described using the nomenclature discussed in Experimental Procedures with the exception of the following terms: GTm (gyrus temporalis medius), GF (gyrus fusiformis), GO (gyrus orbitales). BA indicates the probable Brodman area, for cortical areas, of activation. Under Tal Coordinate are the Talairach coordinates (Talairach and Tournoux, 1988) of the voxel with the maximum p value as determined from the KS maps (Breiter et al., 1996b). Coordinates are expressed in mm from the anterior commissure: R/L, right (+)/left (−); A/P, anterior (+)/posterior (−); S/I, superior (+)/inferior (−). The number of voxels around the max vox that meet the p value threshold of $p < 10^{-6}$ are listed under Vox #. Proximity lists whether the voxels with the maximum p values for each activation are within 1.5 cm of each other; thus a plus sign is placed in the last column if they are <1.5 cm apart, or a minum sign is placed if they are more than 1.5 cm apart.

[a] Indicates there is no overlap, but the max vox of the two activations are within 1.5 cm of each other.

seen in the cocaine maps; only one negative saline signal change, in the superior temporal gyrus, matched the location of an activation with negative signal change following cocaine infusion.

Test–Retest Comparisons

As with the cocaine test–retest comparisons, four of seven subjects had interpretable saline infusion data for test–retest comparison after motion correction. For the saline test–retest comparison with four individuals, no limbic or paralimbic regions were activated. For regions outside of limbic and paralimbic regions, six of the test activations were also similar to those seen with retest. Of these six activations, four of the six approximated activations seen with the average saline map of ten individuals, suggesting that the subgroup of four represent a good approximation of the group of ten.

The saline retest data evidenced multiple new activations not seen during the first saline test. The majority of these (10/16) were in the striate, extrastriate, and ventral temporal cortex implicated in ventral stream information processing for vision (Tootell et al., 1995). Eleven of the sixteen activations were similar to activations seen with the initial cocaine infusion for the total cohort and the retest cocaine infusions in the subgroup of four individuals (Table 5). Most striking was the appearance of activations in the bilateral NAc/SCC (Talairach coordinates: R/L −9, A/P 18, S/I 3; R/L 9, A/P 15, S/I −3) and the right insula (Talairach coordinates: R/L 40, A/P −15, S/I 0). The saline retest NAc/SCC (Figure 7) and insula activations closely approximated the same activations seen for the initial cocaine infusion in the total cohort (see Tables 1–4) and the cocaine NAc/SCC activation that correlated more with maximum ratings of craving than with rush (Tables 1–4). Moreover, these NAc/SCC and insula activations were similar to the same activations in the cocaine condition that showed good cocaine test–retest reproducibility (Table 5). Compared to the bilateral NAc/SCC activations seen with cocaine test–retest infusions, the bilateral NAc/SCC activations seen with saline retest infusion demonstrated a lower percent signal change (left = 0.4%, right = 1.5%) for all voxels meeting the threshold of $p < 10^{-5}$. On the basis of location of activation maxima, 11 of the 16 new activations seen with saline retest infusion in the NAc/SCC, the frontal cortex, and the temporal cortex were seen with either the cocaine test or retest infusions.

Discussion

Following an infusion of cocaine under double-blind conditions, cocaine-dependent subjects demonstrated significant increases in HR and MBP and decreases in $ETCO_2$. Cocaine plasma concentration reached maximum at ~7 min after infusion. Subjects reported early

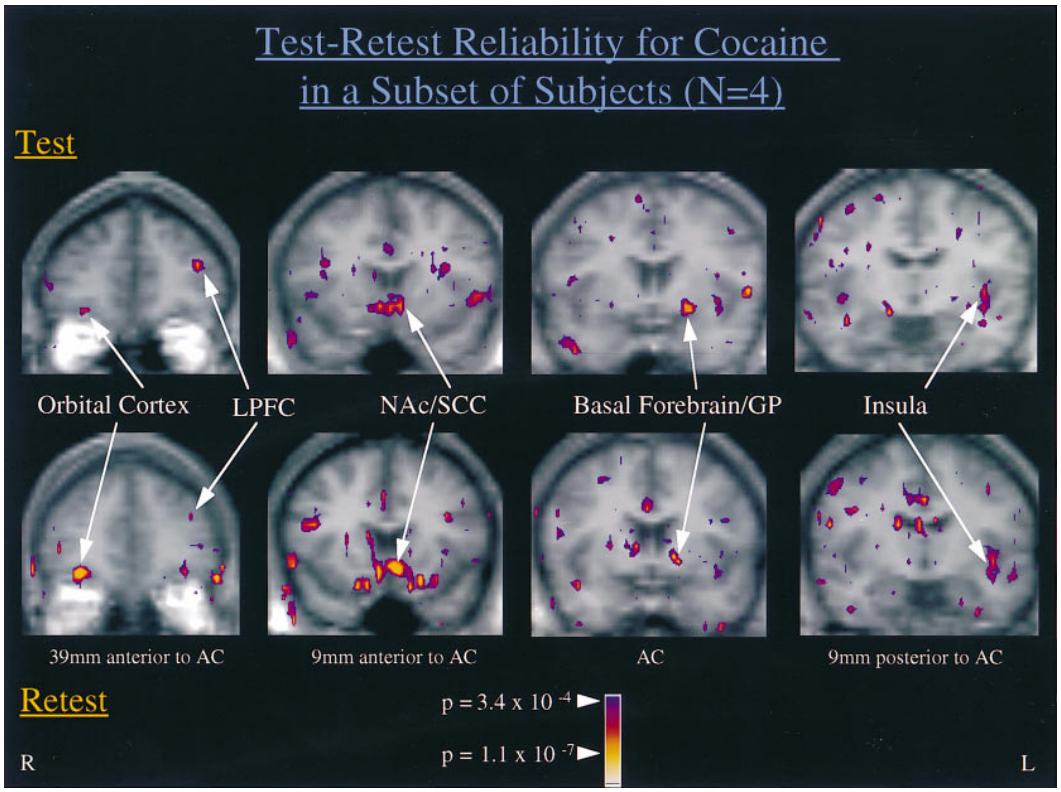

Figure 6. Test–Retest Cocaine Experiments

The Kolmogorov-Smirnov (KS) statistical maps (unsmoothed) for the average fMRI data in Talairach space from four subjects who had test–retest cocaine infusions are displayed in pseudocolor on top of gray scale structural images from these same subjects. Coronal slices are identified by their relationship in mm to the anterior commissure (AC).

maxima ~3 min after infusion for behavioral ratings of rush and high and later maxima for behavioral ratings of craving and low. Thus, maximal subjective euphoria was reported during the distribution phase of cocaine plasma kinetics, before maximal intravascular cocaine levels had been attained.

Brain regions that showed focal increases in BOLD signal at the time of onset of subjective measures of euphoria included putative brain reward circuitry (NAc/SCC, basal forebrain, and VT), caudate, putamen, thalamus, medial temporal and paralimbic regions (hippocampus, parahippocampal gyrus, cingulate cortex, and insula), brainstem (pons), and neocortical regions such as the lateral prefrontal cortex, lateral temporal cortex, parietal cortex, and occipital cortex. Decreases in fMRI signal were also noted in the amygdala, temporal pole, and medial frontal cortex, although the latter regions were in close proximity to areas of susceptibility artifact (see below). In comparison to cocaine, saline produced few regions of fMRI signal increase, limited to lateral prefrontal and temporo-occipital cortex. Small regions of signal decrease were also noted in the lateral prefrontal cortex and temporal cortex. All of the four positive temporal lobe activations seen during the saline infusion, along with the negative temporal pole activation, were also seen in the cocaine condition.

Multiple correlational analysis of averaged behavioral ratings with averaged cocaine fMRI data indicated differences in the temporal pattern of activation, which can be associated with rush and with craving ratings (Figure 8). Brain activation correlated with rush ratings was noted in a subset of regions associated in animal experiments with brain reward such as the VT, left basal forebrain, midbrain and pontine brainstem, bilateral caudate nucleus, and right cingulate gyrus. All of these regions are directly connected with the VT or the nucleus accumbens. Other brain activations in regions not previously implicated in animal models of drug self-administration or BSR, which showed a similar pattern of early transient signal maxima, included regions of prefrontal, parietal, temporal, and occipital cortex. Brain activation correlated with craving measures was noted in the NAc/SCC and right parahippocampus. A negative correlation with craving was also noted in the amygdala (a region with negative fMRI signal change on the average maps).

Limitations

In this study, subjects exhibited head movement following both cocaine and placebo infusions despite use of a bite bar. Complete movement correction was possible for some subjects with maximal displacements up to ~3 mm, although in some subjects, complex movements of similar magnitude produced unacceptable residual motion artifacts. As with our previous experience with a psychiatric population (Breiter et al., 1996b), a significant proportion of studies (6/17 cocaine infusions and 4/15 saline infusions) had to be discarded due to uncorrectable movement.

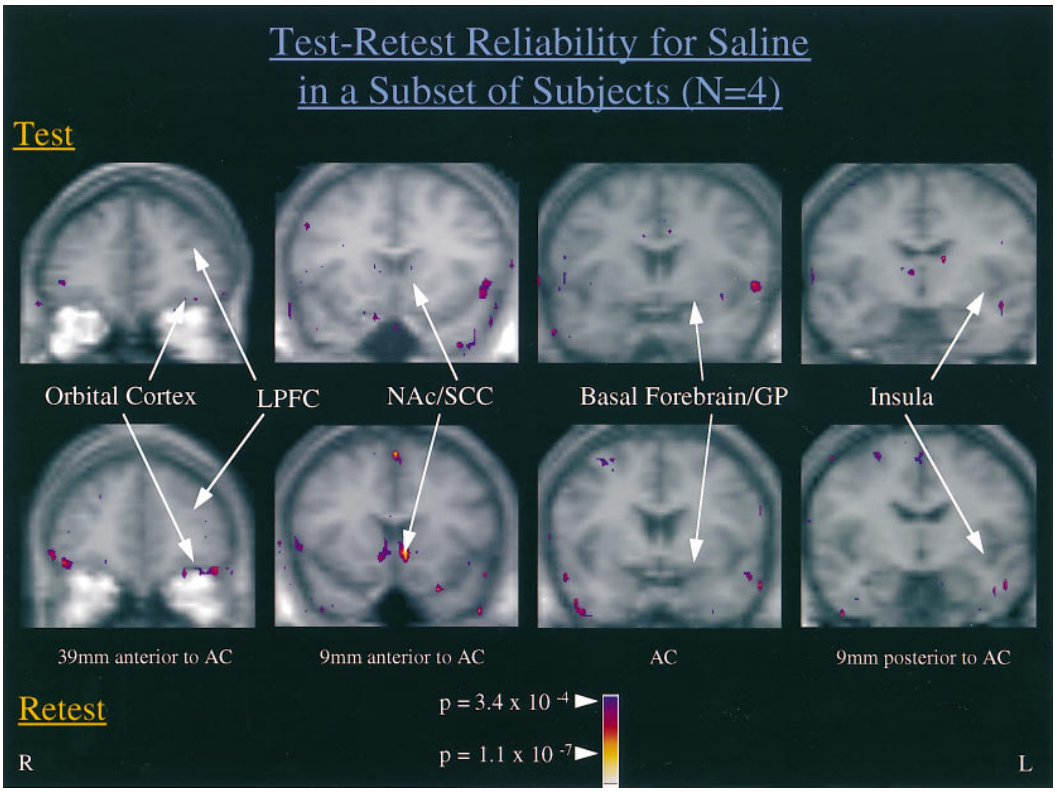

Figure 7. Test–Retest Saline Experiments

The Kolmogorov-Smirnov (KS) statistical maps (unsmoothed) are displayed as described in Figure 6, but for the four subjects who had test–retest saline infusions. Note the NAc/SCC activaton in the cocaine test (Figure 6) but not the saline test condition (this figure). By the retest, NAc/SCC activation could also be observed in response to the saline condition. Despite this generalization of response, NAc/SCC activation still represented a larger percent signal change for both the test and retest cocaine conditions.

Motion correction must also be considered in the context of its contribution to altered spatial resolution. Our voxel size during imaging was 3.125 × 3.125 × 8 mm, which would appear adequate to resolve some subnuclei of larger subcortical structures. But, the combination of (1) motion correction, (2) transformation into Talairach space, and (3) averaging alter our effective spatial resolution to approximately 1 cm^3. Activations from averaged data in our study, thus, cannot be attributed with certainty to specific subnuclei of larger gray matter structures. Indeed, any anatomic localization with averaged data sets and superimposition of different structural and functional data acquisitions must be considered in probabilistic terms. This is the case even for individual statistical maps superimposed on structural images, albeit to a lesser degree, since images are superimposed from different acquisitions with the potential for movement between them, as well as different spatial warping and signal-to-noise characteristics. These issues are apparent with the test–retest data, where some activations that overlap do not necessarily have statistical maxima in the identical anatomic spot. This could be due to limitations imposed by our effective spatial resolution or noise of physiological origin in our underlying fMRI measurements.

Some regions, such as the NAc/SCC, basal forebrain, hypothalamus, and amygdala, are near areas with a high potential for magnetic susceptibility artifact, primarily seen on echo-planar images as signal dropout. Given unpredictable effects on T2*-weighted signal change from regions with high susceptibility, especially with concurrent motion, we checked and confirmed that activations seen with the cocaine and saline infusions did not overlap regions of susceptibility artifact on the functional images. For this reason, regions such as the medial frontal cortex and temporal pole, which showed large negative signal changes that were proximal to areas of susceptibility artifact, cannot be considered reliable activations.

Two issues regarding experimental design need to be mentioned. This study incorporated double-blind conditions and subject instructions designed to equalize cocaine expectancy for each infusion, in both test and retest conditions. Despite these precautions, since subjects knew they would only receive a single infusion per scan and could feel the infusion volume as it was administered, the blind only lasted a few minutes past the infusion, after which all subjects knew whether they had received cocaine or saline. This was clearly reflected, for both test and retest conditions, in the absolutely uniform zero ratings for rush and high following saline.

Secondly, in the design of the overall study, multiple attempts were made to distinguish BOLD fMRI signal

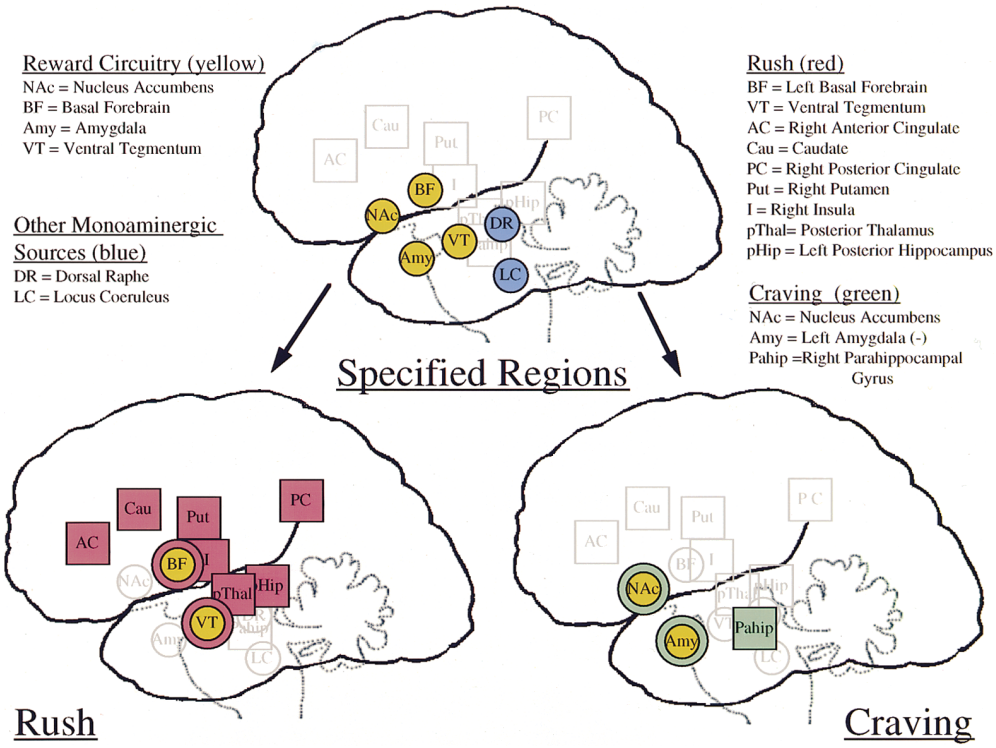

Figure 8. Summary Schematic of Limbic and Paralimbic Brain Regions that Correlate with Euphoria (in Red) Versus Those Regions that Correlate with Craving (in Green)

Above these summary schematics is a schematic of the brain regions (in yellow) we predicted to be active after the infusion of cocaine. Two other brainstem monoaminergic regions, potentially encompassed in a pontine activation seen in our baseline versus postinfusion comparison, are also illustrated in blue. This pontine activation did correlate with behavioral ratings for rush.

changes due to region specific activation from changes due to systemic physiological or direct vascular effects of cocaine. Each infusion scan (see Figure 1) was bracketed by control experiments to determine whether regionally specific primary visual cortex activation was altered by the cocaine or placebo infusion, and how much change there was in global cerebral blood flow (Gollub et al., submitted). The results of these control experiments clearly support our interpretation of focal regional activation following cocaine infusion. Focal primary visual cortical activation was quantitatively unchanged following cocaine or saline. Moreover, although the flow-sensitive scan revealed an approximate 14% decrease in flow-related signal in cortical gray matter, no such change was measured during BOLD scanning. Even with these reassurances, though, a strong caveat should be added to the results of local gray matter changes related to cocaine; namely, that they were observed in the presence of significant cardiovascular and respiratory effects from cocaine.

Finally, a general issue regarding the linkage of fMRI signal to underlying neuronal activity must be mentioned. At this time, the relationship of BOLD signal to pre- and postsynaptic mechanisms of neurotransmission is unknown. Thus, it is conceivable that increased fMRI signal in the NAc/SCC, for example, could be due to increased activity of inhibitory (GABAergic) nerve terminals, which produce a decrease in neuronal cell body activity in the NAc/SCC rather than excitatory input to or output from the NAc/SCC, which would be associated with a regional increase in neuronal cell body activity. The linkage of fMRI signal to underlying neuronal activity remains an area of continuing research, which is needed to connect more directly the results of this neuroimaging study and others to the body of basic substance abuse research using animals.

Regions with Short Duration Signal Change and Relation to Euphoria

Two of the behavioral ratings used in this experiment, rush and high, described separable features of the subjective experience of euphoria or pleasure. Such subjective measures can only be obtained with human subjects. With animal experiments, behavioral scientists have been limited to investigation of the effects of "rewarding" stimuli on observable behavior (White et al., 1987) based on repeated approach behaviors or response repetitions. It can be hypothesized that acutely rewarding behavioral stimuli (i.e., cocaine) administered to a conscious (human) subject produce not only behavioral effects (reinforcement) and lead to encoding of emotional memories but also produce subjective pleasure that can be reported.

Behavioral research with animal models has shown that increased dopamine transmission in the nucleus accumbens is associated with behavioral responses to rewards. However, the exact relationship of mesoaccumbens dopamine function to the action of a reward

as an incentive or as a reinforcement has been an area of controversy (Richardson and Gratton, 1996). The implicit assumption in relating dopamine transmission in the nucleus accumbens to cocaine use is that dopamine transmission is a central correlate of the reinforcing actions of rewards (Wise et al., 1978; Wise, 1982; Koob, 1992). Thus, in humans, we postulated that an acute change in fMRI activation in the nucleus accumbens area (NAc/SCC) would be correlated with behavioral measures of euphoria. The pattern of fMRI signal change could not be predicted, since dopamine produces complex modulatory effects on postsynaptic neurons and because the relationship of the BOLD signal to pre- and postsynaptic mechanisms of neurotransmission is unknown. What we found was that fMRI activation in the VT (the source of dopamine for the nucleus accumbens), basal forebrain, pontine brainstem, caudate, insula, cingulate gyrus, and prefrontal cortex were correlated with behavioral measures of euphoria.

Computational models of the output of VT neurons suggest that they code for a deviation between the experienced reward and the previous predictions for reward. VT neurons would accordingly report ongoing prediction errors for reward and deliver a signal to forebrain targets to alter ongoing processing of reward predictions and the direction of reward-maximizing actions (Schultz et al., 1997). Thus, in the naive state, VT neuronal firing is increased in nonhuman primates early in the acquisition of lever pressing behavior (Schultz, 1986; Nishino et al., 1987; Romo and Schultz, 1990; Schultz and Romo, 1990; Ljungberg et al., 1992; Schultz et al., 1993). However, after several lever press trials in the same experiments, simulating a more chronic state of drug use, VT neurons demonstrate electrophysiological decreases in response. In our fMRI study, subjects were chronic users but were naive to cocaine use in the fMRI environment. They showed a pattern of early but transient signal change in VT, which is analogous to the response of primates naive to cocaine. Perhaps the novelty of cocaine administration in the fMRI setting may have contributed to the observed VT activation. This formulation regarding learning effects could be confirmed by serial retest studies with larger cohorts than our current study.

Regions to which VT input might be important in mediating the subjective concomitants of reward and that demonstrated activation with early signal maxima and short duration and thus correlation with rush ratings include the cingulate gyrus and the basal forebrain. The cingulate gyrus has been associated both with euphoric experiences in humans induced by procaine (Ketter et al., 1996) but also, in direct contrast, with the emotional intensity of aversive events (Talbot et al., 1991; Sikes and Vogt, 1992; Coghill et al., 1994; Casey et al., 1996; Craig et al., 1996). The basal forebrain has also been implicated in affective function, in that it has been directly implicated in the results from BSR experiments. Since BSR was first observed by Olds and Milner (1954), evidence has accumulated that regions such as VT, lateral hypothalamus (Murray and Shizgal, 1991, 1996), and basal forebrain (Rompre and Shizgal, 1986; Shizgal et al., 1989; Arvanitogiannis et al., 1996) contain the neuron somata that generate this effect. It is important to note that the basal forebrain constitutes one of the primary outputs of both the nucleus accumbens and the amygdala (Heimer et al., 1997).

In our study, extensive brainstem activation distinct from the VT was also observed, including activation in the vicinity of regions for other monoaminergic systems such as the serotonergic system (primarily the dorsal raphe) and the noradrenergic system (the locus coeruleus). This other brainstem activation also demonstrated early signal maxima with rapid return to basal levels that correlated with rush ratings. FMRI BOLD scans in the brainstem are confounded by cardiac-induced motion. Thus, replication of our brainstem observations using a recently developed technique of cardiac gating with a subsequent T1 correction algorithm (Guimares et al., 1996) will be important.

Regions of Sustained Signal Change and Possible Relation to Cocaine-Induced Craving

In this study, no brain region showed statistically significant signal intensity changes that directly paralleled the change in behavioral ratings for cocaine-induced craving or dysphoria (i.e., with slow onset of signal change and peak effects after approximately 10 min). To a first approximation, the ramp function of the craving ratings is the same as the average motion displacement detected by the AIR algorithm. Since our baseline drift correction removed signal changes that would be correlated with this motion, the absence of brain regions with time course changes specific for cocaine-induced craving is a matter to be interpreted with caution.

Some brain regions did however show sustained activation that led to a higher degree of correlation with the craving ratings. Our observation, for instance, of sustained signal change in the NAc/SCC is the explanation for its stronger association with craving than with rush ratings. In general, the differences at high thresholds between the rush and craving correlation maps reflect a distinction between behavioral ratings with early peaks and shorter duration (i.e., rush) and ratings with prolonged time courses (i.e., craving; see signal time courses in Figures 3a and 3b). It is significant that subtraction of fMRI time courses with early maxima and short duration from those with prolonged time courses would produce a time course closely resembling that of the craving ratings. This suggests a possible model for craving in humans. Craving may not be mediated by one or two distinct brain regions; rather, postcocaine craving may reflect a change over time in the pattern of brain activation from cocaine. Many brain regions are active at the time that subjects report euphoria. Over time, though, only a few brain regions remain activated; this change in the pattern of brain regions activated may be causally related to the subjective experience of craving.

The observation of sustained activation in the NAc/SCC, which occurred over the time interval that subjects experienced cocaine-induced rush and then craving, links the NAc/SCC with both reinforcement and with incentive functions. This contrasts with the simple view that dopamine transmission in the nucleus accumbens area (NAc/SCC) is the central correlate of reward and therefore subjective euphoria. Although some studies

have reported an association between feeding or consummatory behavior and elevated dopamine levels in the nucleus accumbens (Heffner et al., 1980; Hernandez and Hoebel, 1988; Radhakishun et al., 1988; Yoshida et al., 1992), other studies suggest that the increases in nucleus accumbens dopamine transmission do not result from consummatory behavior (Blackburn et al., 1986, 1989, 1992; Chance et al., 1987; Weatherford et al., 1991; McCullough and Salamone, 1992; Elbaz et al., 1993, Soc. Neurosci., abstract; McCullough et al., 1993; Phillips et al., 1993; Salamone et al., 1994) and that mesoaccumbens dopamine neurons respond to incentive rather than to reinforcing components of rewards (Kiyatkin and Gratton, 1994; Richardson and Gratton, 1996). Our fMRI data, showing a correlation between cocaine-induced craving and sustained activation in the NAc/SCC, supports a complex role for the NAc/SCC in the human, with a potential role in incentive as well as reinforcement.

Other brain regions with sustained signal change after early signal maxima included several lateral prefrontal regions and one section of the parahippocampal gyrus (see Figure 3b), though other parahippocampal activations did not display this behavior (see Tables 1–4). The parahippocampal gyrus has efferents to the nucleus accumbens and amygdala, is a primary input source for the hippocampus, and has been implicated not only in explicit memory (Squire and Knowlton, 1995) but also in the association of context to emotionally relevant stimuli during fear conditioning (LeDoux, 1993). The common sustained activation of the NAc/SCC and parahippocampal gyrus, along with relatively discrete sections of lateral prefrontal cortex, points to a distributed network of brain regions involved with the cocaine-induced craving.

Sustained negative signal change in the left amygdala was also observed. This left amygdala signal change needs to be discussed with the caveat that inspection of individual maps showed some heterogeneity of activation, in that three subjects evidenced positive signal change and only five subjects displayed negative signal change. Such heterogeneity in amygdala activation resembles electrophysiologic findings in rodents, in that acute intravenous cocaine produces mixed suppression and excitation in amygdalar neurons (Cunningham, 1995). In contrast, microiontophoretic application of cocaine in the amygdala uniformly produces suppression of spontaneous neuronal discharges (Cunningham, 1995), indicating that functional connectivity is important for mediating amygdala response to cocaine.

Our left amygdala data appear to contrast with other reports of positive correlation between amygdala activation and cue-elicited craving (Childress et al., 1996, Soc. Neurosci., abstract; Grant et al., 1996; Schweitzer et al., 1996, Soc. Neurosci., abstract). The amygdala has been implicated in the orientation to and remembering of affectively salient stimuli for social interaction (Leonard et al., 1985; Rolls, 1992; Breiter et al., 1996d). Interpretation of our current negative amygdala activation in the context of this other work can only be speculative. It is possible that cocaine-induced craving represents a distinct process from that of cue-conditioned craving (Everitt, 1997). Given the potential for expectancy effects in the current double-blind infusion experiment, order effects in each of the cue-conditioned craving experiments (Childress et al., 1996, Soc. Neurosci., abstract; Grant et al., 1996; Schweitzer et al., 1996, Soc. Neurosci., abstract), and differences in neuroanatomical resolution between our fMRI work and the PET studies of other investigators (Childress et al., 1996, Soc. Neurosci., abstract; Grant et al., 1996; Schweitzer et al., 1996, Soc. Neurosci., abstract), further work will be needed to assert that differences exist between craving during acute cocaine withdrawal and craving elicited by cues.

Signal Changes During Saline and Possible Relation to Expectancy and Craving

The lateral prefrontal and temporo-occipital activations observed with saline infusion were similar to activations after cocaine infusion and might represent a common effect from expectation or a chance similarity given the number of regions activated during the cocaine condition. It is unlikely they represent chance, since they were mostly replicated in saline retest experiments. The saline activations might be considered in the context of the results from a recent PET study of cue-induced cocaine craving in cocaine addicts (Grant et al., 1996), if one considers the saline infusion as a potential cue. In the study of Grant and colleagues (1996), increased glucose metabolism was reported in the lateral prefrontal and temporo-occipital cortices. It is interesting to note the similarity of regional activation between studies, even though our subjects rated craving at zero throughout the saline infusion.

The issue of cocaine expectancy also arises with regard to new activations observed with the saline retest experiments. Orbital cortex activation was noted bilaterally on saline retest; this region has been implicated in the suppression of expectancies in animals (Morgan et al., 1993; Morgan and LeDoux, 1995). Bilateral NAc/SCC activation was also observed with saline retest. Given theorized involvement of the nucleus accumbens with the processing of predictions of reward (Schultz et al., 1997) and observations of altered conditioned responses in animals after only one cocaine dose (Weiss et al., 1989), it is possible the NAc/SCC activation on saline retest may represent one-trial learning. Further work will be needed to evaluate the time course of change in regions such as the NAc/SCC to determine if these represent learning effects (Schultz et al., 1997).

Conclusions

During double-blind infusion experiments in cocaine-dependent subjects, we observed dramatic effects from cocaine in physiology, behavioral report, and fMRI brain activation that were not found following saline. A significant feature of this study was the continuous sampling of brain blood oxygenation changes to intravenous cocaine over 18 min, which was exploited for multiple correlational analysis with the behavioral data. Several brain regions showed short duration of activation that was well correlated with the reinforcement-related rating of rush, while other regions showed sustained activation, demonstrating some of the features associated

with the incentive-related measure of craving. In particular, the VT and basal forebrain correlated more strongly with rush measures, while the NAc/SCC and amygdala correlated more strongly with craving measures, even though these latter two regions had early signal maxima as seen with the rush measures. Early but sustained activation in the NAc/SCC implies that it is activated during both rush and craving experiences, which contrasts with the general view of circuitry mediating reinforcement (Wise et al., 1978; Wise, 1982; Koob, 1992) and suggests the NAc/SCC is also involved with incentive functions.

In contrast to cocaine effects, saline produced activations in prefrontal cortex and lateral temporo-occipital cortex, most of which were also found active with cocaine, and resembled findings from other investigators during cue-induced craving in abstinent cocaine-dependent subjects (Childress et al., 1996, Soc. Neurosci., abstract; Grant et al., 1996; Schweitzer et al., 1996, Soc. Neurosci., abstract). The observation of NAc/SCC activation on saline retest infusion raises the possibility that generalization of expectancy across the two infusion conditions may occur within one trial; this hypothesis needs confirmation.

Our cocaine results provide evidence in the human for a functional integration of circuits involved with reinforcement and circuits involved with drug craving (see Figure 8). The known anatomic interconnections between limbic and paralimbic regions with short duration versus sustained alteration in BOLD signal converge on a core set of brain regions: the NAc/SCC, basal forebrain, amygdala, and VT. From animal research, there is evidence that the VT is necessary for reward prediction (summarized in Schultz et al., 1997), the amygdala for orienting to and remembering affectively significant stimuli (Everitt et al., 1991; LeDoux, 1992; Hatfield et al., 1996) and attentional modulation of perceptional function (Leonard et al., 1985; Rolls, 1992), the nucleus accumbens for determination and modulation of motoric responses toward perceptual stimuli and internal homeostatic needs (Le Moal et al., 1977; Kelley and Stinus, 1985; Fibiger and Phillips, 1986; White, 1986; Blackburn et al., 1989), and the basal forebrain for attention to internal state and attribution of primary reward (Shizgal et al., 1989; Arvanitogiannis et al., 1996). Future research will be important for determining whether or not these regions function in this manner in humans and how these functions produce incentive and reward.

Experimental Procedures

Subjects

Of the 17 subjects who completed the experimental protocol, 13 were men and four were women (mean age = 34.5 ± 4.6 years; education = 12.2 ± 1.6 years; weight = 79.6 ± 17.8 kg; Addiction Severity Index [McLellan et al., 1980] Composite Score [0 to 1.00] on the drug dimension = 0.18 ± 0.13 and on the alcohol dimension = 0.27 ± 0.25; Hamilton Anxiety Scale [0 to 54] 2.94 ± 2.08; Hamilton Depression Scale [0 to 52] 7.53 ± 5.66). All subjects were right-handed. Except for cocaine addiction, they were medically and neurologically normal by physical exam, review of systems, blood work including electrolytes, liver function tests, cell blood count, and toxicology. No subject had a history of head trauma with loss of consciousness or had any family history of sudden cardiac death or cardiac disease. All subjects tested negative for human immunodeficiency virus (HIV). Women were not pregnant by βHCG testing and were scanned at the midfollicular phase of their menstrual cycle. All subjects fulfilled criteria for cocaine dependence, with or without comorbid alcohol or marihuana abuse, by Mini-Structured Clinical Interview for DSM-IV (SCID) (American Psychiatric Association, 1994). Our subjects were selected to be heavy, long-term cocaine users (mean = 7.8 ± 6.0 years; days of cocaine use in 30 days prior to experiment = 16.2 ± 8.2 days). Current monetary expenditure for cocaine was $397.0 ± 318.0 over the week prior to the experiment. No subjects were seeking or receiving treatment for substance abuse at the time of the study. To be accepted into the imaging protocol, during screening, subjects had to have one positive urinalysis to confirm recent cocaine use, but had to be abstinent from cocaine and alcohol for at least 18 hr before the infusion. Approximately 18 hr before each imaging session, subjects underwent a screening IV test dose of 0.2 mg/kg in the MGH Mallinckrodt GCRC under the supervision of a cardiologist and psychiatrist to ascertain cardiac and neurological tolerance of the experimental procedures. They were subsequently monitored in the GCRC until the time of scanning. All subjects gave informed consent to participate in these procedures following the rules of the Subcommittee on Human Studies at MGH. Subjects were reimbursed for participation in this protocol on the basis of days in the hospital and could earn a bonus for completion of all scans. Reimbursement was with noncash vouchers (e.g., nontransferrable food coupons).

Experimental Design

Subjects were admitted to the MGH GCRC for the screening procedures; those meeting all criteria were boarded overnight on the unit in preparation for imaging the following day. The following morning, the subject had bilateral intravenous catheters placed (right forearm for cocaine or saline infusion, left forearm for serial venous blood sampling for quantitative cocaine levels). Scanning was performed between 11 AM and 3 PM, during which the subject was in the scanner for two periods of time, each lasting from 45 to 90 min. During each scanning period, one infusion was given, either cocaine (0.6 mg/kg, maximum dose 40 mg) or saline (both in a volume of 10 ml given over 30 s IV) in a randomized, double-blind order. Five different scans were performed during each period. The infusion itself was made 5 min into an 18-minute-long BOLD scan. The BOLD infusion scan was bracketed by flow-sensitive alternating inversion recovery (FAIR) and visual stimulation BOLD scans (the data from these scans were used to delineate the global versus regional signal changes from cocaine and are reported in a separate manuscript [Gollub et al., submitted]). The time interval between functional scans within a period was kept to a minimum. The entire sequence of five functional scans was completed within 45–60 min. The subject was removed from the scanner for a 15–30 min rest and then was returned to magnet and the sequence was repeated for the second infusion. A minimum of 2 hr had to pass between each double-blind infusion.

Subject Instructions

For the preexperiment test infusion with 0.2 mg/kg cocaine on the night before scanning, subjects were informed they would receive a small dose of intravenous cocaine in the presence of a cardiologist and a psychiatrist to screen for medical side effects from intravenous cocaine and to train them in making behavioral ratings of their experience.

For experiments performed in the magnet, subjects were informed they would receive two infusions to which both they and the experimenters were blind. Infusions could either be saline or 0.6 mg/kg of cocaine in saline; the experience of one infusion did not imply what would be the identity of the other. Subjects were further asked to continue behavioral ratings throughout the FAIR and BOLD infusion scans (~40 min in total) and to remain as motionless as possible to minimize fMRI movement artifacts. All subjects understood they could terminate the experiment at any time without explanation.

Plasma/Urine Monitoring

Sequential 4 ml venous blood samples were collected immediately before and at 1, 3, 5, 10, 15, 30, 60, 90, and 120 min following each

infusion. The 120 min sample for the first infusion was also the preinfusion sample for the second infusion.

Physiological Monitoring

Physiologic monitoring was conducted using an InVivo OmniTrak 3100 patient monitoring system (Orlando, FL) modified to permit on-line computer acquisition of physiologic measurements. Each subject was fitted with chest leads to record the electrocardiogram (ECG) and to measure heart rate (HR), a nasal cannula to measure respiratory rate and $ETCO_2$, and a blood pressure cuff to measure noninvasively systemic MBP. The temporal resolution of the system for sampling blood pressure was once every 2 min. The InVivo system sampled and displayed updated values for each of the other parameters once per second except for the ECG trace, which was digitized at a rate of 100 Hz.

The measured physiologic parameters were ported to a Macintosh Power PC 7100 running a custom National Instruments LabView data acquisition program. This program allowed the simultaneous acquisition of (1) the digitized analog ECG trace signal acquired using a National Instruments MIO16L board, (2) the GE scanner J8 trigger pulse that indicated when the gradient coils of the magnet were firing, and (3) serial port read of ASCII characters reporting physiologic measures from the InVivo system.

Precautions taken to ensure safe conduct of the study included use of ACLS trained personnel, frequent running of mock codes with clocked performance of tasks and strict definition of individual tasks, and presence of a cardiologist at the time of all infusions whose sole responsibility was to monitor subject safety. Before and after completion of both infusions, subjects underwent a 12-lead ECG to determine the absence of any interval change from the experiments and to clear them for discharge home. Because of magnetohydrodynamic effects on the ECG tracing, a baseline rhythm strip was obtained prior to each drug infusion and all subsequent tracings were compared to that one.

Behavioral Monitoring

For both infusions, analog scales for behavioral response were projected via the LabView program and a back projection television system (Sharp Liquid Crystal, RU2000) outside the Faraday shield of the scanner. These projected stimuli were then focused via a biconvex lens (Buhl Optical) inside the Faraday shield onto a rear projection screen that was viewed through an overhead mirror in the magnet bore. For both infusions, subjects viewed images prior to actual experimentation so that images could be focused and centered in each subject's visual field.

During FAIR and BOLD infusion scans, behavioral measures of rush, high, low, and craving were obtained in a continuous sequence each minute. Thus, over each 15 s epoch, one rating scale would be projected for the subject's response. Given four scales, it took 1 min to cycle through the complete set of scales. Timing of scan initiation, infusion onset and offset, and scan completion were linked with ongoing behavioral reports to allow subsequent correlational analysis between behavioral ratings and fMRI acquisitions. Behavioral responses were acquired with a four-button button press that had been adapted to the magnet environment by construction with nonmagnetic components and filtering of its output at the Faraday shield.

To obtain meaningful behavioral ratings during scanning, subjects were trained beforehand. The day before scanning, subjects were interviewed in depth by one of two board-certified psychiatrists to describe fully their experience of cocaine intake. These descriptions were then categorized by the psychiatrist and subject into four components: the rush, high, low, and craving that were to be rated on an integer scale of 0 (none) to 3 (maximum). The individualized conventions for description of subjective responses were then tested, during the unblinded preinfusion with 0.2 mg/kg cocaine, on a portable computer with a program simulating that used in the MRI.

Of the four behavioral measures, only craving was defined operationally in terms of the action the individual wanted to engage in (to get more cocaine). The other three behavioral measures, rush, high, and low, were defined in terms of subjective feelings that were not necessarily associated with a behavioral output or associated with the planning and implementation of physical activity. Thus, by definition, only craving was defined as a motivational state. In general, rush experiences involved physical sensations of elevated heart rate and sweating, along with internal feelings variously characterized as "speeding" sensations and sensations of "being out of control". In contrast, the high experience was generally associated with feelings of self-confidence, well-being, and sociability. The low experience encompassed all negative subjective feelings potentially associated with cocaine use, such as anxiety, paranoia, dysphoria, or anhedonia; the majority of subjects in this study discussed the low in terms of dysphoric effect distinct from a diminishment in the high experience.

Imaging

Scanning was performed with a quadrature head coil and a 1.5 T MR scanner (General Electric) modified for echo-planar imaging (Advanced NMR). Imaging involved the following protocol. First, a sagittal localizer scan (conventional T1-weighted spoiled gradient refocused gradient echo [SPGR] sequence; through-plane resolution = 2.8 mm; 60 slices) was performed to orient, for subsequent scans, 15 contiguous axial slices covering the whole brain. This scan was also used as the structural scan for Talairach transformation. Next, an automated shimming technique was used to optimize B_0 homogeneity (Reese et al., 1995). This was followed by an SPGR T1-weighted flow-compensated scan (resolution = 1.6 mm $\times$ 1.6 mm $\times$ 8 mm), which was primarily obtained to aid Talairach transformation during data analysis (see Breiter et al., 1996b). The fourth scan was a T1-weighted echo-planar inversion recovery sequence (TI = 1200 ms, in-plane resolution = 1.57 mm) for high resolution structural images to be used in preliminary statistical maps but not with Talairach transformed or averaged maps. Finally, BOLD imaging was performed using an asymmetric spin echo T2*-weighted sequence (TR = 8000, TE = 50, 180° refocusing pulse offset by −25 ms; FOV = 40 $\times$ 20 cm; in-plane resolution = 3.125 mm; through-plane resolution = 8 mm; 15 contiguous axial slices covering the whole brain) to measure "activation" (local changes in blood flow and oxygenation) (Bandettini et al., 1992; Kwong et al., 1992; Ogawa et al., 1992). Images were acquired interleaved for 136 time points for each infusion.

Data Analysis

Plasma/Urine Levels

Cocaine quantitative assays were performed by the MGH Clinical Chemistry Laboratory using a liquid chromatography with photodiode array detection method they developed (Puopolo et al., 1992), with minor modifications (flow rate increased from 2.0 to 2.6 ml/min and LCPCN column length increased from 150 to 250 mm). Intra-assay imprecision at 100, 20, and 10 mg/l for cocaine is 5.1%, 5.7%, and 6.6%, respectively.

Physiological Data

The data analysis and graphing program IGOR (WaveMetrics, Inc.) was used to analyze the data. Data were first analyzed by a two-way ANOVA with drug treatment (saline, cocaine) and time of measurement as factors. When significant F values were obtained for one of the physiologic measures, individual time points were compared by posthoc t tests to determine if (and at what times) the change from baseline was significant. The Bonferroni correction for multiple comparisons was used; the criteria for significance at the 0.05 level was $p < 0.007$.

Behavioral Data

The integer output for each behavioral rating was segregated by category of rush, high, low, and craving. For the group data in Figure 2, the 18 measures for each behavioral category obtained during the 18 min BOLD infusion scan were averaged for the nine subjects with both interpretable behavioral data and fMRI data. This averaged data was then utilized in the correlational analysis of the cocaine fMRI data.

BOLD Data for Initial fMRI Experiments and for Test/Retest Experiments

MOTION CORRECTION. To reduce head motion, each subject was positioned using a bite bar, and echo-planar data was motion corrected using an algorithm (Jiang et al., 1995) adapted from Woods et al.

(1992) and described elsewhere (Breiter et al., 1996b). Motion correction of the BOLD saline infusion data revealed an average maximal displacement of 1.8 ± 2.3 mm, resulting in a mean correction per time point of 0.6 ± 0.5 mm. For the cocaine infusion data, there was an average maximal displacement of 1.1 ± 0.7 mm, resulting in a mean correction per time point of 0.6 ± 0.4 mm. After motion correction, time series data were inspected to assure that no data set evidenced residual motion in the form of cortical rim or ventricular artifacts >1 voxel. There was no statistically significant difference in maximal displacement between paired groups of saline versus cocaine infusions ($p < 0.4$).

TALAIRACH TRANSFORMATION. Each individual's set of infusion-related functional images, along with the associated conventional structural scans, were transformed into Talairach space (Talairach and Tournoux, 1988; Breiter et al., 1996b, 1996d) and resliced in the coronal orientation over 57 slices with isotropic voxel dimensions (x, y, z = 3.125 mm). Because of possible movement between acquisitions of structural and functional scans, functional data were further fit to the structural scan by translation of exterior contours. For the cocaine and saline infusions, two subjects evidenced movement between structural and functional scans of >2 voxels in magnitude, and, therefore, were discarded from further analysis.

NORMALIZATION, AVERAGING, AND CONCATENATION. For cocaine and saline infusions, Talairach-transformed functional data were intensity scaled (i.e., normalized relative to a standard preinfusion epoch) so that all mean baseline raw magnetic resonance signals were equal. Talairach-transformed structural and functional data were then averaged by run across the ten subjects with interpretable cocaine infusion data and the ten subjects with interpretable saline infusion data; similar averaging of Talairach-transformed structural and functional data was performed for the four subjects used in the test/retest analysis (Breiter et al., 1995, Proc. Soc. Magn. Reson./Euro. Soc. Magn. Reson. Med. Biol., abstract; Breiter et al., 1995, Proc. Soc. Neurosci., abstract; Brieter et al., 1996b, 1996d).

VOXEL-BY-VOXEL STATISTICAL MAPPING. Unsmoothed Kolmogorov-Smirnov (KS) statistical images were constructed (Breiter et al., 1996b, 1996d) from these averaged data sets comparing baseline (N = 38 time points) and postinfusion (N = 98 time points) epochs. Drift correction (i.e., removal of a first-order linear function) was incorporated in the statistical calculation but not for the signal intensity time courses shown. Subsequently, clusters of activation were determined on data that were smoothed by a 0.7 pixel gaussian filter (∼ Hamming filter in the spatial domain). To guide the determination of activation clusters, smoothed data sets were subjected to a cluster-growing algorithm (Jiang et al., 1996, Neuroimage, abstract; Bush et al., 1996, Neuroimage, abstract) and activation clusters listed that met a corrected p value threshold. The cluster-growing algorithm was set to select activations with maximum p values below $p < 10^{-5}$ and to separate activations with pixels of $p < 10^{-4}$ between them. All activation clusters were then evaluated on the unsmoothed data to ascertain that they met cluster constraints, did not overlap areas of susceptibility, had time courses consistent with the experimental paradigm, and could be anatomically localized (see below for details). The correction for multiple comparisons of this data, in order to maintain an overall $\alpha < 0.05$, was the Bonferroni correction for all gray matter voxels sampled in the brain, or $p < 7.1 \times 10^{-6}$ (Breiter et al., 1996d). To be tabulated, activations had to meet cluster constraints on the unsmoothed KS statistical maps as follows: for subcortical gray matter, three contiguous voxels with one voxel at $p < 7.1 \times 10^{-6}$ and two voxels at $p < 10^{-5}$; and for cortical activations, five contiguous voxels with one voxel at $p < 7.1 \times 10^{-6}$ and four voxels at $p < 10^{-5}$. The effect of such cluster constraints on statistical significance have been discussed previously by our group (Breiter et al., 1996b).

The time course of signal change was evaluated for each putative activation identified on statistical maps of averaged data by the cluster-growing algorithm. These signal intensity versus time curves were assessed to ascertain that activation did not precede infusion onset. All activations had to meet this constraint, along with anatomical constraints that the Talairach coordinate of their maximum voxel (i.e., the voxel with the lowest p value) was in the brain as assessed by the Talairach atlas (Talairach and Tournoux, 1988) and that the activation, when thresholded at $p < 10^{-5}$, did not extend outside the brain when superimposed over the Talairach-transformed structural images.

NEUROANATOMICAL ANALYSIS. We used a combined approach to anatomic localization of functional data. The group average data (GAD) were mapped using an approach focused on Talairach coordinates. In addition, the individual data (ID) were mapped using a region of interest-based approach, focused on the limbic and paralimbic areas.

Anatomic Localization of GAD. Statistical maps of group averaged data were superimposed over high resolution conventional T1-weighted images that had been transformed into the Talairach domain and averaged. Primary anatomic localization of activation foci was performed by inspection of these coronally resliced T1-weighted scans and via the Talairach coordinates of the maximum voxel from each activation cluster (see section on determination of activation clusters). Subcortical localization of activations followed the region of interest conventions described below and demonstrated in Figure 4. All activations were checked against the functional image data to ascertain that they did not overlap areas of susceptibility artifact. Such overlap was determined by whether or not a voxel's signal intensity during the baseline was less than the average voxel in its slice by 50% of the difference between the average voxel signal intensity in the slice and the average voxel signal intensity outside of the slice.

Anatomic Localization of ID. To assess the degree to which subcortical activations seen in the group represent common activations across the population, as opposed to the effect of strong activations in a few subjects, each individual's Talairach-transformed T1 high resolution scan was inspected and regions of interest (ROIs) defined. Visual inspection of the superimposed KS statistical maps, thresholded at a liberal statistical threshold (KS, $p < 0.001$), was then performed to determine if activation was present in each of the anatomic structures discussed below. These results were tabulated as a ratio of individuals showing lateralized activation in that structure to the total number of subjects evaluated (N = 10). As our predictions involved only subcortical structures, our individual analysis also focused on noncortical regions, with the exception of medial paralimbic and intrasylvian cortices.

The methods used for definition of the subcortical ROIs followed the conventions of the MGH Center for Morphometric Analysis. These ROIs were defined by use of specific anatomic landmarks identified by direct visualization of each individual Talairach-transformed T1 anatomic scan. These coronal scans had voxel dimensions of x, y, z = 3.125 mm, a matrix of 49 × 37 × 57, and were viewed on the computer monitor with a size of 38 mm × 31 mm (see Figure 4). Key landmarks necessary for anatomic localization included the anterior commissure (AC), posterior commissure (PC), lateral geniculate nucleus (LGN), mammillary body (MB), substantia nigra (SN), anterior and posterior extents of amygdala, anterior and posterior extents of hippocampus, posterior extent of pulvinar, collateral sulcus, and splenium of corpus callosum.

Sixteen ROIs were defined to encompass the following structures: the caudate nucleus (Cau), the nucleus accumbens and subcallosal cortex (NAc/SCC), the putamen (Put), the pallidum (GP), the amygdala (Amy), the anterior and posterior insula (aINS and pINS), the anterior and posterior hippocampus (aHip and pHip), the parahippocampal gyrus (Parahip), the precommissural and postcommissural cingulate gyrus (aCG and pCG), the basal forebrain (BF), the precommissural and postcommissural thalamus (aThal and pThal), the lateral geniculate nucleus (LGN), and the ventral tegmentum (VT: including SN and surrounding region). Definitions for each of these ROIs were as follows: Cau extents reached from the anterior tip of its head to the part of its body corresponding at the coronal level of the LGN. NAc/SCC was identified at the inferior junction between the head of Cau and the Put. It was delimited superiorly by a line connecting the inferior corner of the lateral ventricle and the inferiormost point of the internal capsule abutting NAc/SCC and laterally by a vertical line passing from the latter point. Put, GP, VT, LGN, and Amy were directly visualized, and the posterior extent of Amy was at the identical coronal plane as the anterior tip of aHip. The posterior extent of the aHip was the coronal plane in front of the PC; the PC plane was the anterior border of pHip. The posterior border of the pHip was identified by direct visualization. Parahip was limited superiorly by the hippocampus or the amygdala and inferiorly by the collateral sulcus. By convention, we did not consider Parahip activation behind the posterior end of the hippocampus.

The insula was directly identified on the coronal plane throughout its anteroposterior extent; its anterior portion (aINS) continued to the coronal plane before the AC while its posterior extent (pINS) included the coronal plane with the AC. The precommissural cingulate (aCG) extended from the paracingulate sulcus anteriorly to the coronal plane anterior to the posterior commissure. Its superior border was determined by the paracingulate sulcus through the coronal slice containing the AC and, behind this plane, the cingulate sulcus. Its inferior border was defined by the paracingulate sulcus (curving portion) anteriorly and the callosal sulcus posteriorly. The postcommissural cingulate (pCG) extended from the coronal plane of the PC anteriorly to the subparietal sulcus posteriorly. Its superior border was defined by the cingulate sulcus and the subparietal sulcus, whereas its inferior border was the anterior portion of the calcarine sulcus (Damasio, 1995; Caviness et al., 1996). BsFor region extended anteroposteriorly from the NAc level to the SN coronal section and medially to the hypothalamus (which extended anteroposteriorly from AC to include posteriorly the MB, having a vertical line at the level of the optic tract or the lateralmost extent of the optic chiasm of the internal capsule as its lateral border and the interhemispheric midline as its medial border). The thalamus was divided anteroposteriorly in two sectors. The aThal extended from the anterior tip of the thalamus to the coronal plane anterior to the posterior commissure, and pThal extended posterior to the PC, including the PC coronal section. The thalamic ROIs were defined inferiorly by the hypothalamic fissure.

Correlational Analysis of BOLD Data from the FMRI Experiments

A multiple correlational analysis was performed between group-averaged behavioral data (N = 9), and group-averaged fMRI data (N = 10). In one subject, the behavioral data was not time locked to the scanner due to computer malfunction, thus these data were not used in the group average of behavioral data. The multiple correlation technique involved cross-correlation of the group average behavioral ratings for rush and craving with the group average fMRI data to generate correlation coefficient (R value) maps and transformation of the R value maps via the Fischer transform into p value maps. To be tabulated, an activation had to have five contiguous voxels with $R > 0.70$ for each voxel. For 136 time points, an $R > 0.70$ corresponds to a $p < 10^{-20}$. Because we averaged ten subjects, this $R > 0.70$ corresponds to an $R > 0.22$ in the individual. The resultant maps illustrated the brain regions whose signal change resembled the time course of rating change for each category of subjective rating.

Comparison of BOLD Data from Test Experiments with Retest Experiments

For the subgroups of subjects that had interpretable repeat cocaine infusion scan data (N = 4) and those with interpretable repeat saline infusion scan data (N = 4), data analysis involving Talairach transformation, signal normalization, averaging, and statistical mapping followed the procedures described above. Also, as above, activations were determined using the same cluster-growing algorithm; activations were interrogated regarding proximity to susceptibility, relationship to experimental paradigm, and anatomy in similar manner. Activations were tabulated with the number of unsmoothed voxels in each activation cluster that met the criteria of $p < 10^{-6}$. Similarity of activation between test and retest conditions was determined by the proximity of the maximum voxels (i.e., with reference to p value threshold) for each activation and by overlap between the set of voxels in each cluster that met the threshold of $p < 10^{-6}$ (note: the Bonferroni threshold for multiple comparisons is $p < 7.1 \times 10^{-6}$). To be considered "similar" activations, they had to have their maximum voxels within 1.5 cm of each other or have at least one overlapping voxel at the strict $p < 10^{-6}$ threshold.

Acknowledgments

This work was supported by grants to H. C. B., R. L. G., and B. R. R. from the National Institute of Drug Abuse (grants #00265, #00275, and #09467) and to B. R. R. from the Heart, Lung, and Blood Institute of the NIH (grant #39810), Bethesda, Maryland. This work was also supported by a Young Investigator Award to H. C. B. from the National Alliance for Research on Schizophrenia and Depression (NARSAD).

We thank Terry Campbell and Mary Foley for technical assistance, Drs. Peter Fox, Nora Volkow, Anna-Rose Childress, Ron Hammer, and Steve Grant for critical review of the pilot data for this study, Drs. Joseph Coyle and Barry Kosofsky for critical comments on the manuscript, the clinical staff of the MGH GCRC for their clinical and technical assistance, Dr. Verne Caviness for consultation regarding anatomic localization of activation foci, Dr. Alex Guimares for technical assistance initiating these experiments, along with Monica Strauss, Elizabeth Huffman, Etienne Benson and William Kennedy for assistance with data analysis and manuscript preparation.

Received August 22, 1997; revised September 8, 1997.

References

Amaral, D.G., Price, J.L., Pitkanen, A., and Carmichael, S.T. (1992). Anatomical organization of the primate amygdala complex. In The Amygdala, J.P. Aggleton, ed. (New York: John Wiley-Liss), pp. 1–66.

American Psychiatric Association. (1994). DSM-IV: Diagnostic and Statistical Manual of Mental Disorders, 3rd Ed. Rev. (Washington, DC: American Psychiatric Association).

Apicella, P., Ljungberg, T., Scarnati, E., and Schultz, W. (1991). Responses to reward in monkey dorsal and ventral striatum. Exp. Brain Res. *85*, 491–500.

Arvanitogiannis, A., Waraczynski, M., and Shizgal, P. (1996). Effects of excitotoxic lesions of the basal forebrain on MFB self-stimulation. Physiol. Behav. *59*, 795–806.

Bandettini, P.A., Wong, E.C., Hinks, R.S., Tikofsky, R.S., and Hyde, J.S. (1992). Time course EPI of human brain function during task activation. Magn. Reson. Med. *25*, 390–397.

Blackburn, J., Phillips, A., Jakubovic, A., and Fibiger, H. (1986). Increased dopamine metabolism in the nucleus accumbens and striatum following consumption of a nutritive meal but not a palatable non-nutritive saccharine solution. Pharmacol. Biochem. Behav. *25*, 1095–1100.

Blackburn, J., Phillips, A., Jakubovic, A., and Fibiger, H. (1989). Dopamine and preparatory behavior: II. a neurochemical analysis. Behav. Neurosci. *103*, 15–23.

Blackburn, J., Pfaus, J., and Phillips, A. (1992). Dopamine functions in appetitive and defensive behaviors. Prog. Neurobiol. *3*, 247–279.

Breiter, H.C., Berke, J.D., Kennedy, W.A., Rosen, B.R., and Hyman, S.E. (1996a). Activation of striatum and amygdala during reward conditioning: an fMRI study. NeuroImage *3*, S220.

Breiter, H.C., Rauch, S.L., Kwong, K.K., Baker, J.R., Weisskoff, R.M., Kennedy, D.N., Kendrick, A.D., Davis, T.L., Jiang, A., Cohen, M.S., et al. (1996b). Functional magnetic resonance imaging of symptom provocation in obsessive-compulsive disorder. Arch. Gen. Psychiatry *53*, 595–606.

Breiter, H.C., Gollub, R., Weisskoff, R., Kennedy, W., Kantor, H., Gastfriend, D., Berke, J., Riorden, J., Matthew, T., Makris, N., et al. (1996c). Activation of human brain reward circuitry by cocaine observed using fMRI. Proc. Soc. Neurosci. *3*, 1933.

Breiter, H.C., Etcoff, N.L., Whalen, P.J., Kennedy, W.A., Rauch, S.L., Buckner, R.L., Strauss, M.M., Hyman, S.E., and Rose, B.R. (1996d). Response and habituation of the human amygdala during visual processing of facial expression. Neuron *17*, 875–887.

Brown, E.E., Robertson, G.S., and Fibiger, H.C. (1992). Evidence for conditional neuronal activation following exposure to a cocaine-paired environment: role of forebrain limbic structures. J. Neurosci. *12*, 4112–4121.

Casey, K.L., Minoshima, S., Morrow, T.J., and Koeppe, R.A. (1996). Comparison of human cerebral activation pattern during cutaneous warmth, heat pain, and deep cold pain. J. Neurophysiol. *76*, 571–581.

Caviness, V.S., Meyer, J., Makris, N., and Kennedy, D.N. (1996). MRI-based topographic parcellation of human neocortex: an anatomically specified method with estimate of reliability. J. Cog. Neurosci. *8*, 566–587.

Chance, W.T., Foli-Nelson, T., Nelson, J.L., and Fischer, J.E. (1987). Neurotransmitter alterations associated with feeding and satiety. Brain Res. *416*, 228–234.

Coghill, R.C., Talbot, J.D., Evans, A.C., Meyer, E., Gjedde, A., Bushnell, M.C., and Duncan, G.H. (1994). Distributed processing of pain and vibration by the human brain. J. Neurosci. *14*, 4095–4108.

Craig, A.D., Reiman, E.M., Evans, A., and Bushnell, M.C. (1996). Functional imaging of an illusion of pain. Nature *384*, 259–260.

Cunningham, K.H. (1995). Modulation of serotonin function by acute and chronic cocaine: neurophysiological analyses. In The Neurobiology of Cocaine, R.P. Hammer, ed. (Boca Raton, FL: CRC Press), pp. 121–143.

Damasio, H. (1995). Human Brain Anatomy in Computerized Images. (Oxford: Oxford University Press).

DeWit, H., and Wise, R.A. (1977). Blockade of cocaine reinforcement in rats with the dopamine receptor blocker pimozide, but not with the noradrenergic blockers phentolamine or phenoxybenzamine. Can. J. Psychol. *31*, 195–203.

Everitt, B.J. (1997). Craving cocaine cues: cognitive neuroscience meets drug addiction research. Trends Cogn. Sci. *1*, 1–2.

Everitt, B.J., Morris, K.A., O'Brien, A., and Robbins, T.W. (1991). The basolateral amygdala-ventral striatal system and conditioned place preference: further evidence of limbic-striatal interactions underlying reward-related processes. J. Neurosci. *42*, 1–18.

Fibiger, H., and Phillips, A. (1986). Reward, motivation, cognition: psychobiology of neotelencephalic dopamine systems. In Handbook of Physiology: The Nervous System, Vol. 4, V.B. Mountcastle, F.E. Bloom, and S.R. Geiger, eds. (Bethesda, MD: American Physiological Society), pp. 647–675.

Fischman, M.W., and Schuster, C.R. (1982). Cocaine self-administration in humans. Fed. Proceed. *41*, 241–246.

Fischman, M.W., Schuster, C.R., Javaid, J., Hatano, Y., and Davis, J. (1985). Acute tolerance development to the cardiovascular and subjective effects of cocaine. J. Pharm. Exper. Ther. *235*, 677–682.

Foltin, R.W., and Fischman, M.W. (1991). Smoked and intravenous cocaine in humans: acute tolerance, cardiovascular and subjective effects. J. Pharm. Exper. Ther. *257*, 247–261.

Fowler, J.S., Volkow, N.D., Wolf, A.P., et al. (1989). Mapping cocaine binding sites in human and baboon brain in vivo. Synapse *4*, 371–377.

Gaffan, D., and Harrison, S. (1987). Amygdalectomy and disconnection in visual learning for auditory secondary reinforcement by monkeys. J. Neurosci. *7*, 2285–2292.

Gaffan, D., and Harrison, S. (1988). Disconnection of the amygdala from visual association cortex impairs visual reward-association learning in monkeys. J. Neurosci. *8*, 3144–3150.

Gawin, F.H. (1991). Cocaine addiction: psychology and neurophysiology. Science *251*, 1580–1586.

Gollub, R., Breiter, H., Weisskoff, R., Kennedy, W., Kantor, H., Gastfriend, D., Berke, J., Riorden, J., Matthew, T., Makris, N., et al. (1996). Global responses to cocaine during fMRI do not obscure regional activation. Proc. Soc. Neurosci. *3*, 1933.

Graham, J.H., and Porrino, L.J. (1995). Neuroanatomical basis of cocaine self-administration. In The Neurobiology of Cocaine, R.P. Hammer, ed. (New York: CRC Press, Inc.), pp. 3–14.

Grant, S., London, E., Newlin, D., Villemagne, V., Liu, X., Contoreggi, C., Phillips, R., and Margolin, A. (1996). Activation of memory circuits during cue-elicited cocaine craving. Proc. Natl. Acad. Sci. USA *93*, 12040–12045.

Guimares, A.R., Melcher, J.R., Talavage, T.M., Baker, J.R., Rosen, B.R., and Weisskoff, R.M. (1996). Detection of inferior colliculus activity during auditory stimulation using cardiac gated functional MRI with T1 correction. NeuroImage *3*, S9.

Hammer, R.P., Young, B.B., and Thomas, W.L. (1995). Regional metabolic manifestations of cocaine sensitization, tolerance, and withdrawal. In The Neurobiology of Cocaine, R.P. Hammer, ed. (New York: CRC Press, Inc.), pp. 15–29.

Hatfield, T., Han, J.-S., Conley, M., Gallagher, M., and Holland, P. (1996). Neurotoxic lesions of basolateral, but not central, amygdala interfere with pavlovian second-order conditioning and reinforcer devaluation effects. J. Neurosci. *16*, 5256–5265.

Heffner, T., Hartman, J., and Seidan, L. (1980). Feeding increases dopamine metabolism in the rat brain. Science *208*, 1168–1170.

Heimer, L., Harlan, R.E., Alheid, G.F., Garcia, M.M., and DeOlmos, J. (1997). Substantia innominata: a notion which impedes clinical-anatomical correlations in neuropsychiatric disorders. Neuroscience *76*, 957–1006.

Hernandez, L., and Hoebel, B. (1988). Food reward and cocaine increase extracellular dopamine in the nucleus accumbens as measured by microdialysis. Life Sci. *42*, 1705–1712.

Hyman, S.E. (1996). Addiction to cocaine and amphetamine. Neuron *16*, 901–904.

Ito, N., Ishida, H., Miyakawa, F., Naito, H. (1974). Microelectrode study of projections from the amygdaloid complex to the nucleus accumbens in the cat. Brain Res. *67*, 338–341.

Jiang, A., Kennedy, D.N., Baker, J.R., Weisskoff, R.M., Tootell, R.B.H., Woods, R.P., Benson, R.R., Kwong, K.K., Brady, T.J., Rosen, B.R., and Belliveau, J.W. (1995). Motion detection and correction in functional MR imaging. Hum. Brain Mapp. *3*, 1–12.

Johanson, C.E., and Fischman, M.W. (1989). The pharmacology of cocaine related to its abuse. Pharmacol. Rev. *41*, 3–52.

Jones, B., and Mishkin, M. (1972). Limbic lesion and the problem of stimulus-reinforcement association. Expl. Neurol. *36*, 362–377.

Kelley, A., and Stinus, L. (1985). Disappearance of hoarding behavior after 6-hydroxydopamine lesions of the mesolimbic dopamine neurons and its reinstatement with L-dopa. Behav. Neurosci. *99*, 531–545.

Ketter, T., Andreason, P., George, M., Lee, C., Gill, D., Parekh, P., Willis, M., Herscovitch, P., and Post, R. (1996). Anterior paralimbic mediation of procaine-induced emotional and psychosensory experiences. Arch. Gen. Psychiatry *53*, 59–69.

Kiyatkin, E., and Gratton, A. (1994). Electrochemical monitoring of extracellular dopamine in nucleus accumbens of rats lever-pressing for food. Brain Res. *652*, 225–234.

Koob, G.F. (1992). Neurobiological mechanisms of cocaine and opiate dependence. In Addictive States, C.P. O'Brien and J.H. Jaffe, eds. (New York: Raven Press), pp. 171–191.

Koob, G.F. (1996). Drug addiction: the yin and yang of hedonic homeostasis. Neuron *16*, 893–896.

Koob, G.F., and Bloom, F.E. (1988). Cellular and molecular mechanisms of drug dependence. Science *242*, 715–723.

Kwong, K.K., Belliveau, J.W., Chesler, D.A., Goldberg, I.E., Weiskoff, R.M., Poncelet, B.P., Kennedy, D.N., Hoppel, B.E., Cohen, M.S., Turner, R., et al. (1992). Dynamic magnetic resonance imaging of human brain activity during primary sensory stimulation. Proc. Natl. Acad. Sci. USA *89*, 5675–5679.

LeDoux, J.E. (1992). Emotion and the amygdala. In The Amygdala: Neurobiological Aspects of Emotion, Memory, and Mental Dysfunction, J.P. Aggleton, ed. (New York: John Wiley-Liss), pp. 339–351.

LeDoux, J.E. (1993). Emotional memory: in search of systems and synapses. Ann. N Y Acad. Sci. *702*, 149–157.

Le Moal, M., Stinus, L., Simon, H., Tassin, J., Thierry, A., Blanc, G., Glowinski, J., and Cardo, B. (1977). Behavioral effects of a lesion in the ventral mesencephalic tegmentum: evidence for involvement of A10 dopaminergic neurons. In Advances in Biochemical Psychopharmacology, Vol. 16, E. Costa and G.L. Gessa, eds. (New York: Raven Press), pp. 237–245.

Leonard, C.M., Rolls, E.T., Wilson, F.A.W., and Baylis, G.C. (1985). Neurons in the amygdala of the monkey with responses selective for faces. Behav. Brain Res. *15*, 159–176.

Ljungberg, T., Apicella, P., and Schultz, W. (1992). Responses of monkey dopamine neurons during learning of behavioral reactions. J. Neurophysiol. *67*, 145–163.

London, E.D., Cascella, N.G., Wong, D.F., Phillips, R.L., Dannals, R.F., Links, J.M., Herning, R., Grayson, R., Jaffe, J.H., and Wagner, H.N. (1990). Cocaine-induced reduction of glucose utilization in human brain. Arch. Gen. Psychiatry *47*, 567–574.

Louilot, A., Taghzouti, K., Simon, H., and Le Moal, M. (1989). Limbic system, basal ganglia and dopaminergic neurons. Brain Behav. Evol. *33*, 157–161.

Lyons, D., Friedman, D.P., Nader, M.A., and Porrino, L.J. (1996). Cocaine alters cerebral metabolism within the ventral striatum and limbic cortex of monkeys. J. Neurosci. *16*, 1230–1236.

McCullough, L., and Salamone, J. (1992). Involvement of nucleus accumbens dopamine in the motor activity induced by periodic food presentation: a microdialysis and behavioral study. Brain Res. *592*, 29–36.

McCullough, L., Cousins, M., and Salamone, J. (1993). The role of nucleus accumbens dopamine in responding on a continuous reinforcement operant schedule: a neurochemical and behavioral study. Pharmacol. Biochem. Behav. *46*, 581–586.

McLellan, A.T., Luborsky, L., and Woody, G.E. (1980). An improved diagnostic evaluation instrument for substance abuse patients: the addiction severity index. J. Nerv. Ment. Disord. *168*, 26–33.

Mirenowicz, J., and Schultz, W. (1996). Preferential activation of midbrain dopamine neurons by appetitive rather than aversive stimuli. Nature *379*, 449–451.

Morgan, M.A., and LeDoux, J.E. (1995). Differential contribution of dorsal and ventral medial prefrontal cortex to the acquisition and extinction of conditioned fear in rats. Behav. Neurosci. *109*, 681–688.

Morgan, M.A., Romanski, L.M.., and LeDoux, J.E. (1993). Extinction of emotional learning: contribution of medial prefrontal cortex. Neurosci. Lett. *163*, 109–113.

Murray, B., and Shizgal, P. (1991). Anterolateral lesions of the medial forebrain bundle increases the frequency threshold for self-stimulation of the lateral hypothalamus and ventral tegmental area in the rat. Psychobiology *19*, 135–146.

Murray, B., and Shizgal, P. (1996). Attenuation of medial forebrain bundle reward by anterior lateral hypothalamic lesions. Behav. Brain Res. *75*, 33–47.

Nishino, H., Ono, T., Muramoto, K., Fukuda, M., and Sasaki, K. (1987). Neuronal activity in the ventral tegmental area during motivated bar press feeding in the monkey. Brain Res. *413*, 302–313.

Ogawa, S., Tank, D.W., Menon, R., Ellermann, J.M., Kim, S.G., Merkle, H., and Ugurbil, K. (1992). Intrinsic signal changes accompanying sensory stimulation: functional brain mapping using MRI. Proc. Natl. Acad. Sci. USA *89*, 5951–5955.

Olds, J., and Milner, P.M. (1954). Positive reinforcement produced by electrical stimulation of septal area and other regions of rat brain. J. Comp. Physiol. Psychol. *47*, 419–427.

Pearlson, G.D., Jeffery, P.J., Harris, G.J., Ross, C.A., Fischman, M.W., and Camargo, E.E. (1993). Correlation of acute cocaine-induced changes in local cerebral blood flow with subjective effects. Am. J. Psych. *150*, 495–497.

Phillips, A., Atkinson, L., Blackburn, J., and Blaha, C. (1993). Increased extracellular dopamine in the nucleus accumbens of the rat elicited by a conditional stimulus for food: an electrochemical study. Can. J. Physiol. Pharmacol. *71*, 387–393.

Puopolo, P.R., Chamberlin, P., and Flood, J.G. (1992). Detection and confirmation of cocaine and cocaethylene in serum emergency toxicology specimens. Clin. Chem. *38*, 1838–1842.

Radhakishun, F., van Ree, J., and Westerink, B. (1988). Scheduled eating increases dopamine release in the nucleus accumbens of food-deprived rats as assessed with on-line brain dialysis. Neurosci. Lett. *85*, 351–356.

Reese, T.G., Davis, T.L., and Weisskoff, R.M. (1995). Automated shimming at 1.5T using echo planar image frequency maps. J. Magn. Reson. Imaging *5*, 739–745.

Richardson, N., and Gratton, A. (1996). Behavior-relevant changes in nucleus accumbens dopamine transmission elicited by food reinforcement: an electrochemical study in rat. J. Neurosci. *16*, 8160–8169.

Ritz, M.C., Lamb, R.J., Goldberg, S.R., and Kuhar, M.J. (1987). Cocaine receptors on dopamine transporters are related to self-administration of cocaine. Science *237*, 1219–1223.

Rolls, E.T. (1992). Neurophysiology and function of the primate amygdala. In The Amygdala: Neurobiological Aspects of Emotion, Memory, and Mental Dysfunction, J.P. Aggleton, ed. (New York: John Wiley-Liss), pp. 143–165.

Romo, R., and Schultz, W. (1990). Dopamine neurons in the monkey midbrain: contingencies of responses to acute touch during self-initiated arm movements. J. Neurophysiol. *63*, 592–606.

Rompre, P.-P., and Shizgal, P. (1986). Electrophysiological characteristics of neurons in forebrain regions implicated in self-stimulation of the medial forebrain bundle in the rat. Brain Res. *364*, 338–349.

Russchen, F.T., Bakst, I., Amaral, D.G., and Price, J.L. (1985). The amygdalostiatal projections in the monkey. An anterograde tracing study. Brain Res. *329*, 241–257.

Salamone, J., Cousins, M., McCullough, L., Carriero, D., and Berkowitz, R. (1994). Nucleus accumbens dopamine release increases during instrumental lever pressing for food but not free food consumption. Pharmacol. Biochem. Behav. *49*, 25–31.

Schultz, W. (1986). Responses of midbrain dopamine neurons to behavioral trigger stimuli in the monkey. J. Neurophysiol. *56*, 1439–1461.

Schultz, W., and Romo, R. (1990). Dopamine neurons of the monkey midbrain: contingencies of responses to stimuli eliciting immediate behavioral reactions. J. Neurophysiol. *63*, 607–624.

Schultz, W., Apicella, P., Scarnati, E., and Ljungberg, T. (1992). Neuronal activity in monkey ventral striatum related to the expectation of reward. J. Neurosci. *12*, 4595–4610.

Schultz, W., Apicella, P., and Ljungberg, T. (1993). Responses of monkey dopamine neurons to reward and conditioned stimuli during successive steps of learning a delayed response task. J. Neurosci. *13*, 900–913.

Schultz, W., Dayan, P., and Montague, P.R. (1997). A neural substrate of prediction and reward. Science *275*, 1593–1599.

Shizgal, P., Schindler, D., and Rompre, P.-P. (1989). Forebrain neurons driven by rewarding stimulation of the medial forebrain bundle in the rat: comparison of psychophysical and electrophysiological estimates of refractory periods. Brain Res. *499*, 234–248.

Sikes, R.W., and Vogt, B.A. (1992). Nociceptive neurons in area 24 of rabbit cingulate cortex. J. Neurophysiol. *68*, 1720–1732.

Spiegler, B.J., and Mishkin, M. (1981). Evidence for the sequential participation of inferior temporal cortex and amygdala in the acquisition of stimulus-reward associations. Behav. Brain Res. *3*, 303–317.

Squire, L.R., and Knowlton, B.J. (1995). In The Cognitive Neurosciences, M.S. Gazzaniga, ed. (Cambridge, MA: MIT Press), pp. 825–837.

Stein, E.A., and Fuller, S.A. (1992). Selective effects of cocaine on regional cerebral blood flow in the rat. J. Pharmacol. Exp. Ther. *262*, 327–334.

Stein, E.A., and Fuller, S.A. (1993). Cocaine's time action profile on regional cerebral blood flow in the rat. Brain Res. *626*, 117–126.

Talairach, J., and Tournoux, P. (1988). C0-planar Stereotaxic Atlas of the Human Brain (New York: Thieme Medical Publishers).

Talbot, J.D., Marrett, S., Evans, A.C., Meyer, E., Bushell, M.C., and Duncan, G.H. (1991). Multiple representations of pain in human cerebral cortex. Science *251*, 1355–1358.

Tootell, R.B.H., Reppas, J.B., Kwong, K.K., Malach, R., Born, R.T., Brady, T.J., Rosen, B.R., and Belliveau, J.W. (1995). Functional analysis of human MT and related visual cortical areas using magnetic resonance imaging. J. Neurosci. *15*, 3215–3230.

Volkow, N.D., Fowler, J.S., Wolf, A.P., Schlyer, D., Chyng-Yann, S., Alpert, R., Dewey, S., Logan, J., Bendriem, B., Christman, D., et al. (1990). Effects of chronic cocaine abuse on postsynaptic dopamine receptors. Am. J. Psychiatry *147*, 719–724.

Volkow, N.D., Fowler, J.S., and Wolf, A.P. (1991). Changes in brain glucose metabolism in cocaine dependence and withdrawal. Am. J. Psychiatry *148*, 621–626.

Volkow, N.D., Hitzemann, R., and Wang, G.-J. (1992). Long-term frontal brain metabolic changes in cocaine abusers. Synapse *11*, 184–190.

Volkow, N.D., Fowler, J.S., and Wang, G.-J. (1993). Decreased dopamine D2 receptor availability is associated with reduced frontal metabolism in cocaine abusers. Synapse *14*, 169–177.

Volkow, N.D., Wang, G.-J., Fischman, M.W., Foltin, R.W., Fowler, J.S., Abumrad, N.N., Vitkun, S., Logan, J., Gatley, S.J., Pappas, N., et al. (1997a). Relationship between subjective effects of cocaine and dopamine transporter occupancy. Nature *386*, 827–830.

Volkow, N.D., Wang, G.-J., Fowler, J.S., Logan, J., Gatley, S.J., Hitzemann, R., Chen, A.D., Dewey, S.L., and Pappas, N. (1997b). Decreased striatal dopaminergic responsiveness in detoxified cocaine-dependent subjects. Nature *386*, 830–833.

Weatherford, S., Greenberg, D., Melville, L., Jerome, C., Gibbs, J., and Smith, G. (1991). Failure to detect increases in brain dopamine metabolism in rats sham feeding sucrose and corn oil. Pharmacol. Biochem. Behav. *39*, 1025–1028.

Weiss, S.R.B., Post, R.M., Pert, A., Woodward, R., and Murman, D. (1989). Context-dependent cocaine sensitization: differential effect of haloperidol on development versus expression. Pharmacol. Biochem. Behav. *34*, 655.

White, N. (1986). Control of sensorimotor function by dopaminergic nigrostriatal neurons: influence on eating and drinking. Neurosci. Biobehav. Rev. *10*, 15–36.

White, N.M., Messier, C., and Carr, G.D. (1987). Operationalizing and measuring the organizing influence of drugs on behavior. In Methods of Assessing the Reinforcing Properties of Abused Drugs, M.A. Bozarth, ed. (New York: Springer-Verlag), pp. 591–617.

Williams, G.V. (1989). Neuronal activity in the primate caudate nucleus and ventral striatum reflects the association between stimuli determining behavior. In Neural Mechanisms in Disorders of Movement, A.R. Crossman and M.A. Sambrook, eds. (London: John Libbey), pp. 63–73.

Wise, R.A. (1982). Neuroleptics and operant behavior: the anhedonia hypothesis. Behav. Brain Sci. *5*, 39–87.

Wise, R., Spinder, J., DeWit, H., and Gerber, G. (1978). Neuroleptic-induced "anhedonia" in rats: pimozide blocks the reward quality of food. Science *201*, 262–264.

Woods, R.P., Cherry, S.R., and Mazziotta, J.C. (1992). Rapid automated algorithm for aligning and reslicing PET images. J. Comput. Assist. Tomogr. *16*, 620–633.

Yim, C.Y., and Mogenson, G.J. (1982). Response of nucleus accumbens neurons to amygdala stimulation and its modification by dopamine. Brain Res. *239*, 401–415.

Yoshida, M., Yokoo, H., Mizoguchi, K., Kawahara, H., Tsuda, A., Nishikawa, T., and Tanaka, M. (1992). Eating and drinking cause increased dopamine release in the nucleus accumbens and ventral tegmental area in the rat: measurement by in vivo microdialysis. Neurosci. Lett. *139*, 73–76.